AD-A067 266 COMMUNICATIONS RESEARCH CENTRE OTTAWA (ONTARIO) F/G 17/7
RECEIVING ANTENNAS FOR THE NAVSTAR GLOBAL POSITIONING SYSTEM,(U)
OCT 78 R MILNE

UNCLASSIFIED CRC-1319 NL

| OF |
AD
A067266

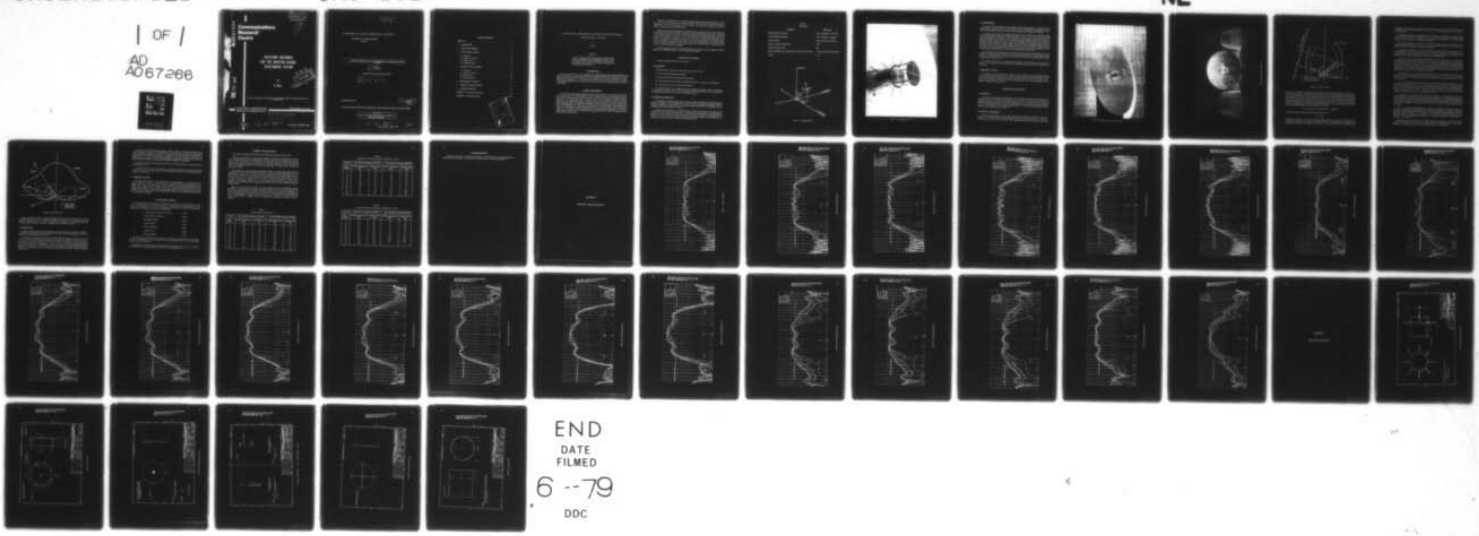

END
DATE
FILMED
6 -79
DDC

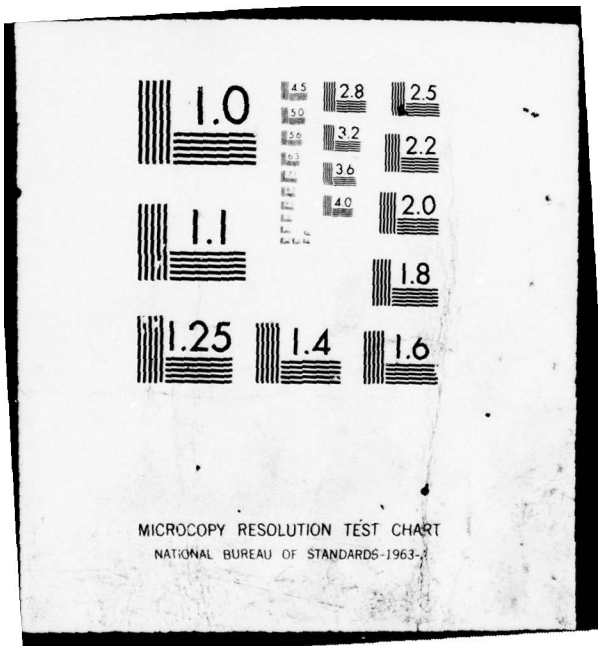
1.0
1.1
1.25
1.4
1.6
1.8
2.0
2.2
2.5
2.8
3.2
3.6
4.0
4.5
5.0
5.6
MICROCOPY RESOLUTION TEST CHART
NATIONAL BUREAU OF STANDARDS-1963-A

Communications Research Centre

RECEIVING ANTENNAS FOR THE NAVSTAR GLOBAL POSITIONING SYSTEM

by

R. Milne

This work was sponsored by the Department of National Defence, Research and Development Branch under Project No. 32E02.

DEPARTMENT OF COMMUNICATIONS
MINISTÈRE DES COMMUNICATIONS

CRC REPORT NO. 1319

CANADA

OTTAWA, OCTOBER 1978

(12) 45p.

COMMUNICATIONS RESEARCH CENTRE

DEPARTMENT OF COMMUNICATIONS
CANADA

(6) # RECEIVING ANTENNAS FOR THE NAVSTAR GLOBAL POSITIONING SYSTEM

by

(10) R. Milne

(Space Technology and Applications Branch)

(14) CRC-1319

CRC REPORT NO. 1319

(11) Oct[illegible]78
OTTAWA

This work was sponsored by the Department of National Defence, Research and Development Branch under Project No. 32E02.

TABLE OF CONTENTS

ABSTRACT 1

1. INTRODUCTION 1

2. DESIGN REQUIREMENTS 1

3. HYBRID SPIRAL ANTENNA 2

   3.1 Description 2
   3.2 Principle of Operation 2
   3.3 Measurements 5
   3.4 Mechanical Design 5

4. COMPOSITE ARRAY ANTENNA 5

   4.1 Description 5
   4.2 Principle of Operation 5
   4.3 Measurements 10
   4.4 Mechanical Design 11

5. MEASUREMENT ACCURACY 11

6. SUMMARY AND CONCLUSIONS 12

7. ACKNOWLEDGEMENTS 14

APPENDIX A – Selected Antenna Patterns 15

APPENDIX B – Mechanical Drawings 36

RECEIVING ANTENNAS FOR THE NAVSTAR GLOBAL POSITIONING SYSTEM

by

R. Milne

ABSTRACT

Two new types of shaped beam receiving antennas have been designed and developed at the Communications Research Centre for the NAVSTAR Global Positioning System. This report contains a description of the antennas, their principles of operation and their measured radiation patterns.

1. INTRODUCTION

This work was carried out for the Department of National Defence under task number 32E02. The objective was to design and develop receiving antennas for the NAVSTAR Global Positioning System. Antenna designs for aircraft, land and sea applications were investigated. This study was complicated by a lack of detailed antenna specifications. For this reason certain assumptions have been made by the author with regards to performance requirements. As a result of this work two new types of receiving antennas have been designed and developed.

2. DESIGN REQUIREMENTS

In the NAVSTAR Global Positioning System a number of satellites travel in 12 hour orbits inclined at 63° to the equatorial plane. They transmit signals to mobile terrestrial receiving systems which use the information to accurately locate their position. Ideally the antennas of the receiving systems should be capable of receiving signals over a 2 π steradians solid angle, i.e. above the local horizon. The antennas are required to exceed a given gain within a specified solid angle. Low ellipticity ratios are required within this angle to minimize the effects of spurious signals that are reflected and diffracted by objects in proximity to the antenna. These signals have random polarization and a phase that is constant relative to the direct signal over the passband of the receiver. Low sidelobe levels are required below the local horizon to minimize the effect of the antenna support structure and to discriminate against multipath signals. A minimum frequency bandwidth and a maximum V.S.W.R. are also specified. As the required angular coverage approaches 2 π steradians, the magnitude of the design problem increases rapidly.

Three types of receiving system in the NAVSTAR Global Positioning System are designated X, Y and Z. The X and Y systems operate at two frequencies, namely 1227 MHz and 1575 MHz with instantaneous bandwidths of 3%. The Z system operates only at 1575 MHz. These systems will be installed on a number of different types of aircraft, land vehicles and ships.

Although the electrical requirements of the receiving systems are likely to be similar, their environmental requirements are quite different. Aircraft in particular provide a difficult operational environment. The presence of large metallic structures in the vicinity of the antenna complicates the electrical design. Not only must the antenna meet the electrical requirements, it must not seriously alter the aerodynamic characteristics of the aircraft. The magnitude of the problem increases as the size of the aircraft decreases. The mechanical interface between the antenna and aircraft must also be simple to avoid major structural changes to the aircraft. Because of a lack of detailed specifications for the receiving antennas of the NAVSTAR system, the design goals listed in Table 1, were used as approximate guidelines.

To satisfy the various electrical and mechanical requirements, two types of antenna, designated "HYBRID SPIRAL" and "COMPOSITE ARRAY", have been designed and developed.

3. HYBRID SPIRAL ANTENNA

The antenna co-ordinate system is shown in Figure 1.

3.1 DESCRIPTION

The antenna consists essentially of 4 elements as shown on Plate 1, namely:

(1) A cavity backed Archimedian Planar Spiral.

(2) Eight radial elements around the periphery of the spiral.

(3) A crossed pair of parasitic elements situated above and parallel to the plane of the planar spiral.

(4) A support structure for the crossed parasitic elements.

The physical dimensions of the antenna are given in the accompanying drawings as shown in Appendix B. The 4 support posts shown on Plate 1 have been replaced by a thin-walled dielectric cylinder. This would be the support structure most likely to be used in an operational antenna.

3.2 PRINCIPLE OF OPERATION

The crossed-pair of parasitic elements are cut to have an inductive impedance at the lowest frequency of operation, i.e. greater than $\lambda/2$. The radial elements are also cut to have an inductive impedance at the lowest frequency of operation, i.e. greater than $\lambda/4$. The parasitic elements are spaced one half wavelength from the planar spiral at the lowest frequency of operation.

The electric field re-radiated by the parasitic elements is almost in antiphase with the incident electric field. Because of the physical separation between the spiral and the elements, the signals received directly and indirectly by the spiral, subtract at zenith and add on the horizon. By this means the E_ϕ elevation pattern is shaped. In a similar manner, use is made of the relative phase difference between the field radiated by the radial elements and that at the spiral to modify the E_θ elevation pattern.

TABLE 1

Design Goals

Parameters	Design Goal
Upper NAVSTAR Frequencies	1575 ± 20 MHz (X, Y, Z systems)
Lower NAVSTAR Frequencies	1227 ± 20 MHz (x, Y systems)
Angular Coverage	zenith to 10° above the horizon
Minimum Circularly Polarized Gain	0 dbi
Maximum Ellipticity Ratio	6 db
Maximum Sidelobe level for angles greater than 20° below the horizon	-15 dbi (measured on a power basis)
VSWR	<1.5

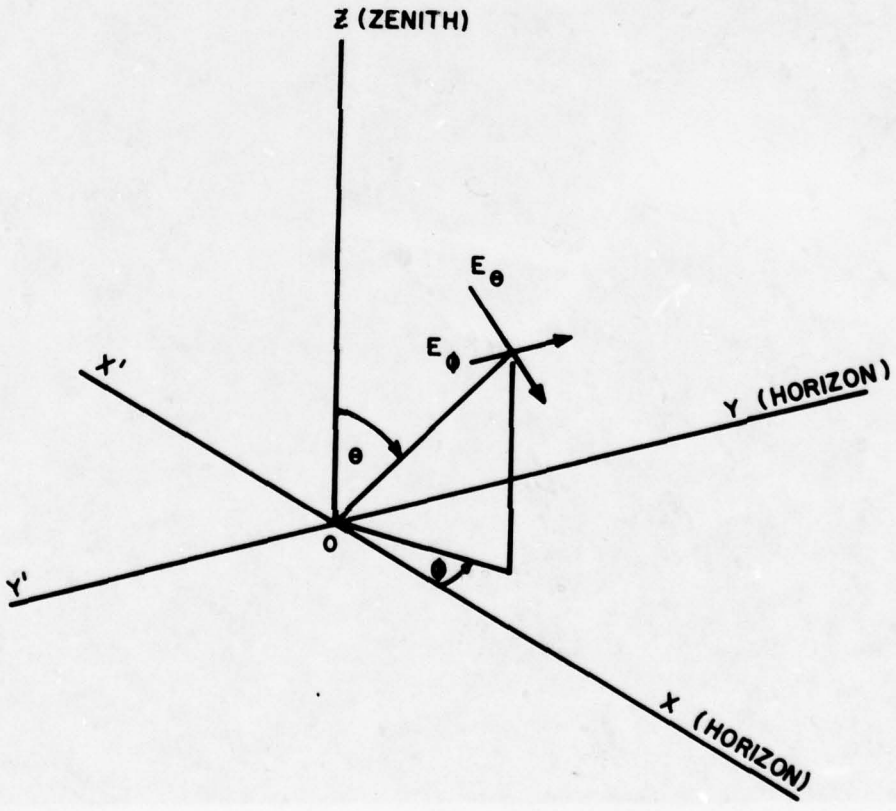

Figure 1. Co-ordinate System

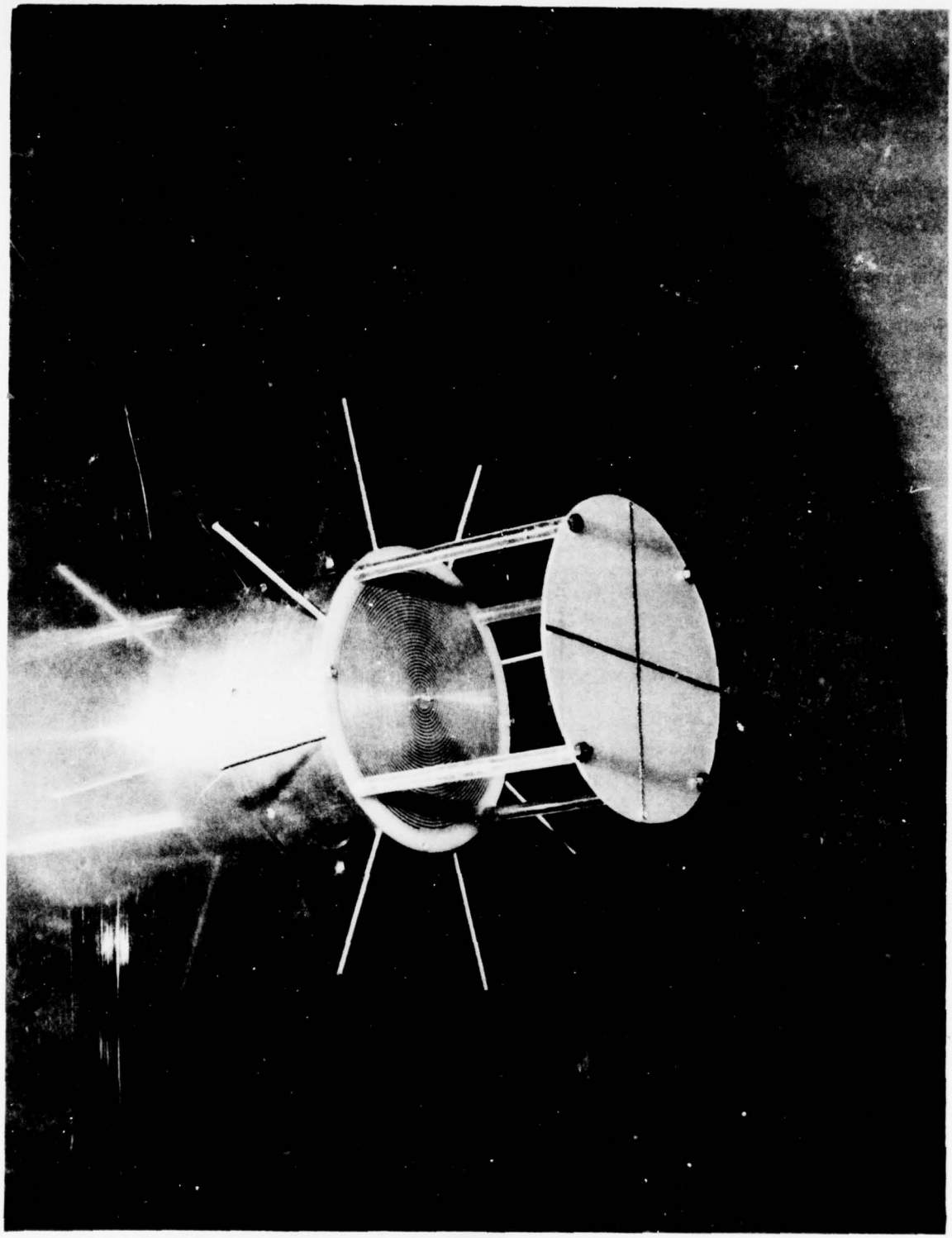

Plate 1. Hybrid Spiral Antenna

3.3 MEASUREMENTS

To simplify the data presentation and highlight significant design parameters, a selected number of antenna patterns measured at the same azimuth angle are included in Appendix A. A complete data package including antenna patterns measured at a number of azimuth angles may be obtained from the author.

The antenna was tested on a 5' diameter ground plane as shown on Plate 2. The antenna has a shaped beam from 1225 MHz to 1662.5 MHz (Appendix A, patterns 1, 5, 9, 13, 17 and 21). The antenna patterns were measured using linear polarization. The polarization vector was rotated in discrete steps of 30°. This provided considerably more information on the antenna's polarization characteristics than the usual method of continuous rotation. Checks were made to ensure that the ellipticity ratios measured were actually the maximum values. At 1575 MHz, a minimum circularly polarized gain of 0 dbi was obtained between zenith and 10° above the horizon, with a maximum ellipticity ratio of 5 dB. At 1225 MHz, a minimum circularly polarized gain of 0 dbi was obtained between zenith and 18° above the horizon with a peak ellipticity of 7 dB. The patterns are symmetrical about the Z axis and almost independent of azimuth angle.

To determine the effect of ground plane size, the antenna was tested on an 18" diameter ground plane (Appendix A, patterns 25 and 26). There is no significant change in gain within the desired angular coverage, but there is an expected increase in sidelobe level. In general, it can be said that the sidelobe level will improve as the ground plane increases in size.

A V.S.W.R. of less than 1.5 was measured across the band. An external balun was used to feed the antenna. In an operational antenna, the balun would be made from microstrip and would be an integral part of the antenna.

3.4 MECHANICAL DESIGN

The antenna has a cylindrical form with a height of 7" and a diameter of 6". The mechanical interface with the aircraft consists of a single hole for the feed cable and 8 small mounting holes around the periphery of the antenna flange. No mechanical analysis has been carried out but if a dielectric cylinder is used to support the parasitic elements, the antenna will have high mechanical strength. The antenna components are relatively simple and easy to manufacture.

4. COMPOSITE ARRAY ANTENNA

4.1 DESCRIPTION

To achieve the required electrical performance, a unique beam-shaping technique has been devised. The technique consists of surrounding an omni-directional type antenna with an array of short vertical dipole elements and an array of short horizontal dipole elements. The arrays are supported by two thin-walled dielectric shells which play no part in the beam shaping process. Two prototype shells with their respective arrays and an omni-directional type antenna are shown in Plate 3. The geometry of the beam shaping structure and its co-ordinate system are shown in Figure 2.

4.2 PRINCIPLE OF OPERATION

The beam shaping technique is most easily described by considering the operation of each array separately. Let the incident plane wavefront directional vector make an angle α with the Z axis. It is desired to increase the gain of the antenna in this direction. As the incident wavefront passes through the convex surface

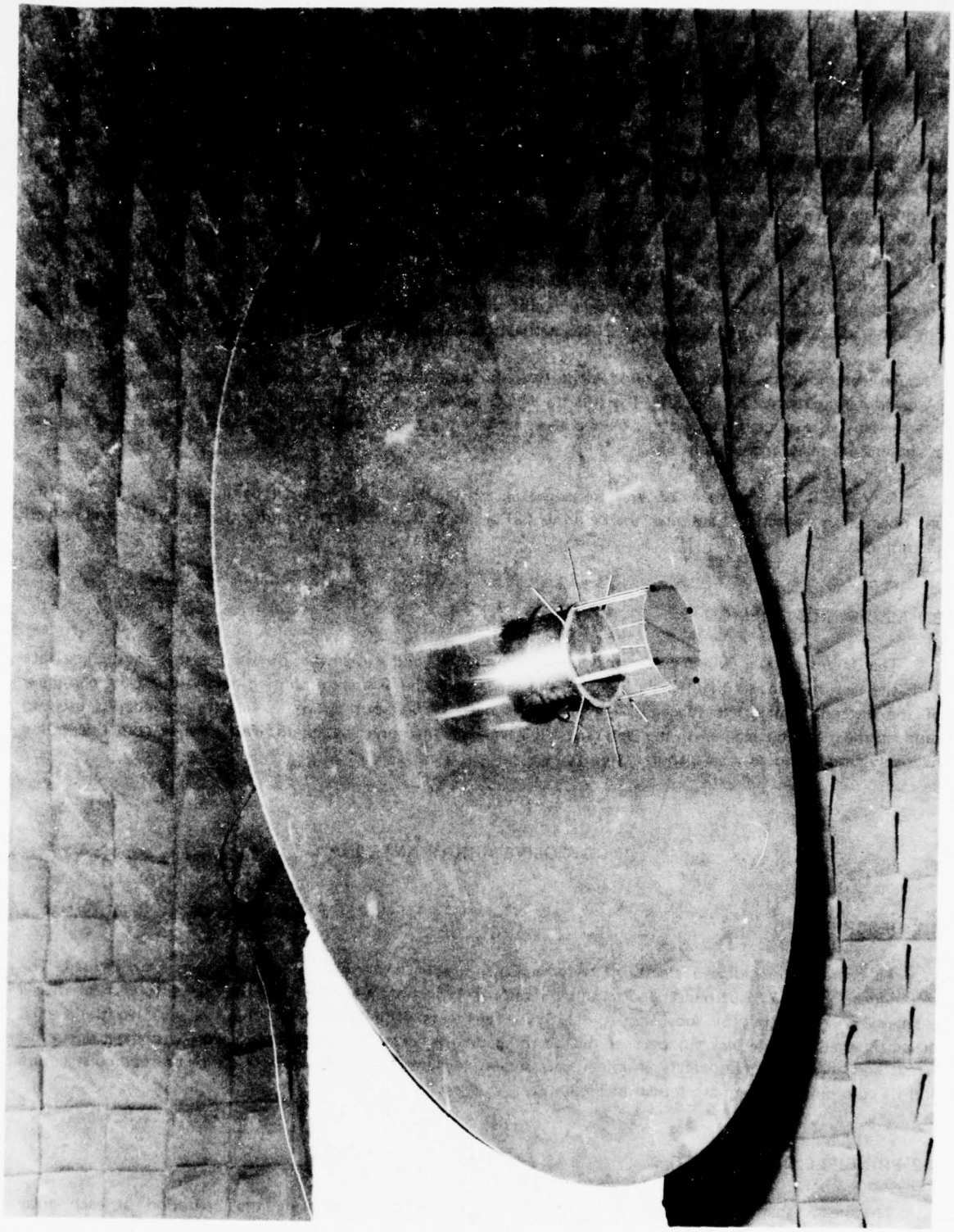

Plate 2. Hybrid Spiral on a 5′ Dia. Ground Plane

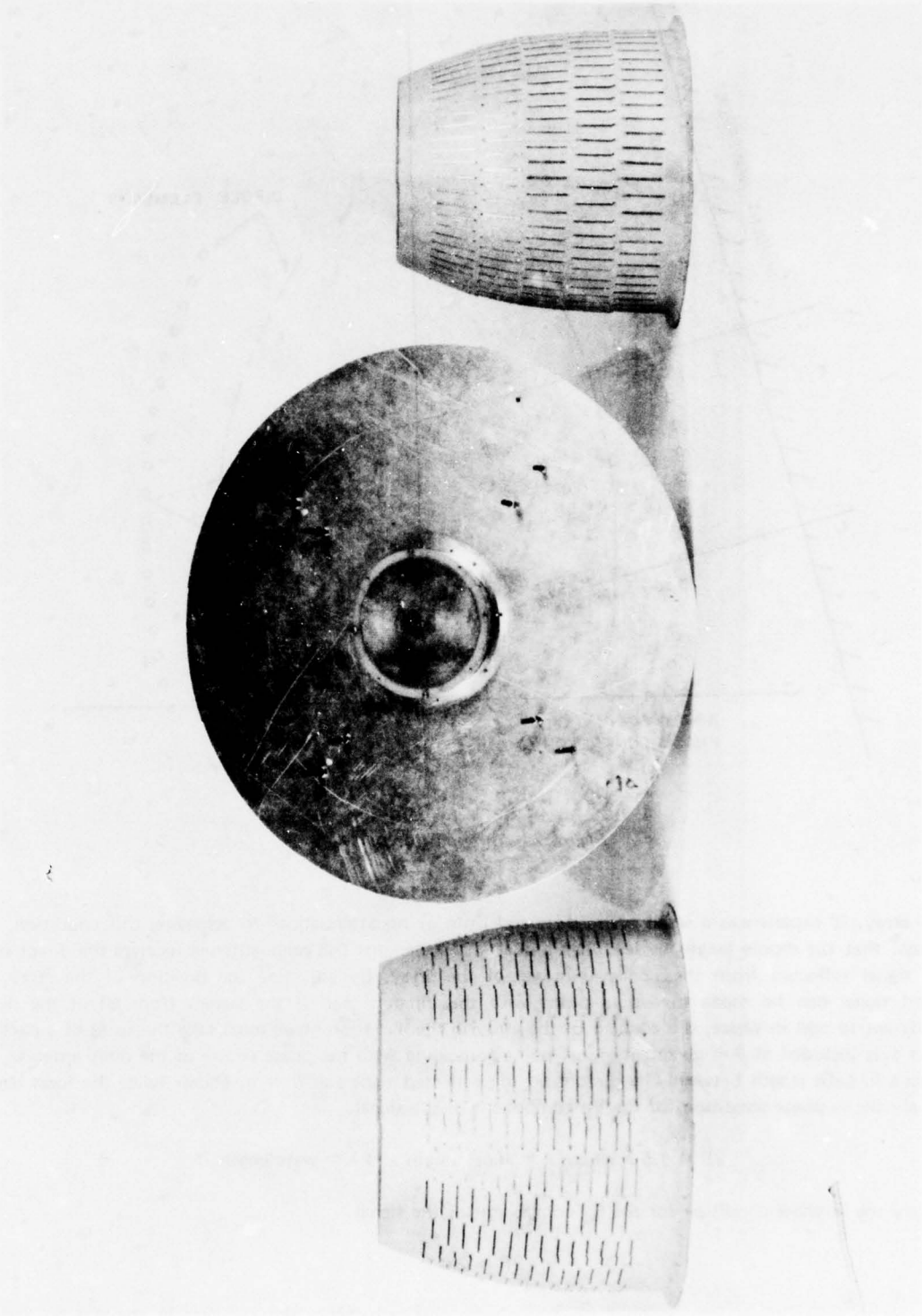

Plate 3. Composite Array Antenna

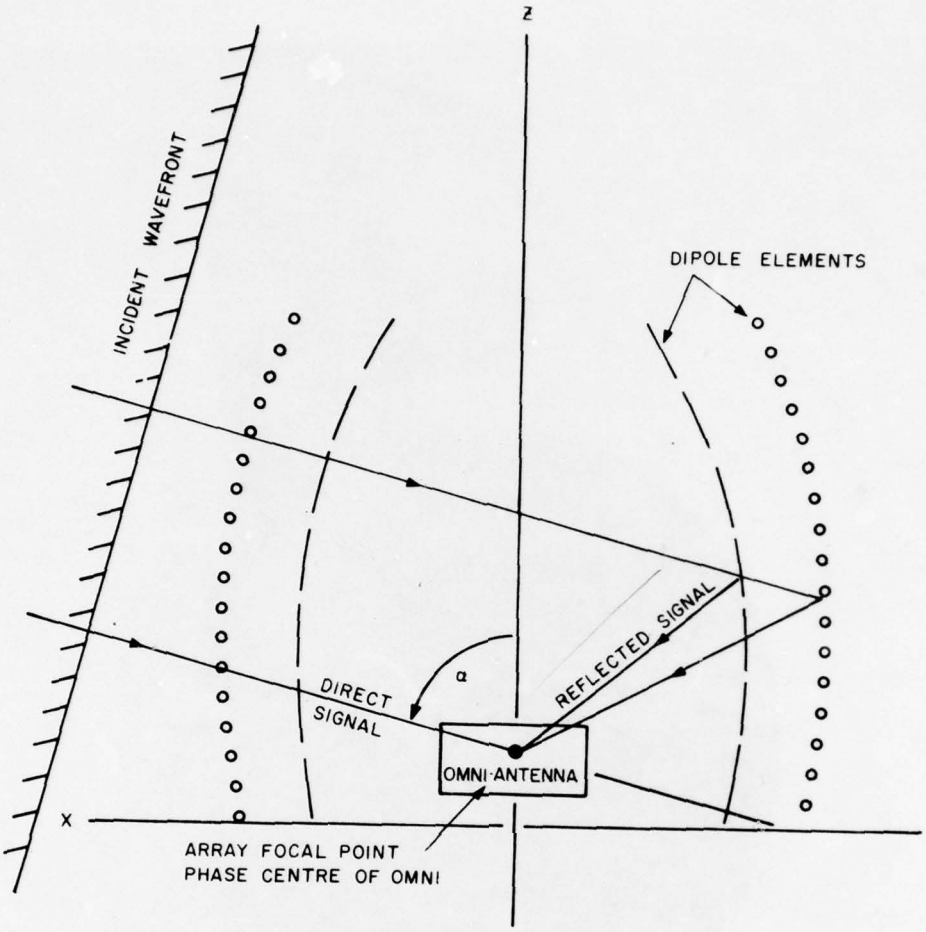

Figure 2. Antenna Geometry

of the array, it experiences a small phase shift and little or no attenuation. In achieving this condition, it is important that the dipole length be less than a quarter wavelength. The omni-antenna receives the direct signal and a signal reflected from the concave surface of the array. By adjusting the position of the array, the reflected signal can be made to add in phase with the direct signal. If the signals from all of the dipole elements are to add in phase, the contour of the array in the elevation plane must take the form of a parabola with its axis included at $\theta = \alpha$, and its focal point coinciding with the phase centre of the omni-antenna. The difference in path length between the direct and the reflected signals at $\theta = \alpha$, equals twice the focal length. To satisfy the in-phase condition for the E_θ component of the signal

$$2F = 1.5\ \lambda \text{ where } F = \text{focal length and } \lambda = \text{wavelength}$$

To satisfy the in-phase condition for the E_ϕ component of the signal

$$2F = 2.0\ \lambda$$

The above formulae takes into account the phase relationship between the currents in the dipoles and the incident electric fields, and the phase relationships between the orthogonal polarization vectors at the omni-antenna. The electric field radiated by the dipoles is in phase with the incident electric field. The E_θ

components of the direct and reflected signals are in antiphase at the omni-antenna. The formulae do not take into account the small phase shift between the direct and the reflected signals introduced by the presence of the dielectric shells.

To satisfy both conditions, two parabolic arrays are required with the orientation of their dipoles aligned to their respective polarization vectors. Both arrays have a common focal point and axis and have circular symmetry about the Z axis. The symmetry of the structure and the orthogonality of the dipole elements permit each array to function almost independently of the other.

The reflection coefficient of each array is a function of the dipole length (L), its width (W), and the separation between the dipoles (S). To achieve a high level of polarization discrimination by the arrays, it is important that the L/W and the S/W ratios be as large as possible.

The dipole array functions as an inclined, off-set parabolic reflector. The gain of the parabolic array is directly proportional to the reflection coefficient of the array and the effective area of the array over which the incident wave is planar. The beam width of the array in the elevation plane is inversely proportional to the effective height of the array which is related almost directly to its physical height.

To illustrate the beam shaping process, the array pattern has been superimposed on an omni-antenna cardioid antenna pattern (Figure 3). The height of the array is chosen to obtain the required array beam width. It is assumed that the gain is to be maximized at $\theta = \alpha$. The height also determines the effective area of the array. The length, width, and spacing of the dipole elements are chosen to obtain the required reflection coefficient. The effective area of the array and the reflection coefficient determine the gain of the array in the direction of $\theta = \alpha$. If the signals received via the array and by the omni-antenna are equal for example at $\theta = \alpha$, the composite pattern will have a 6 dB improvement in gain.

At angles less than $\theta = \alpha$, the reflected signal will lead the direct signal. For angles greater than $\theta = \alpha$, the reflected signal will lag the direct signal. At some angle on either side of $\theta = \alpha$, i.e. at $\theta \pm \beta$, the direct and reflected signals will be in antiphase. The reflected signals will however be attenuated because of the directivity of the array pattern.

In the case of the cardioid omni-antenna pattern, the gain increases as θ decreases. The gain of the array decreases for angles less than α. At $\theta = \alpha - \beta$, the relative difference in gains between the omni-antenna and the array will be appreciable, and there will be a relatively small reduction in gain in the composite antenna pattern. The gain of the cardioid pattern decreases as θ increases. The gain of the array also decreases as θ increases for angles greater than α. At $\theta = \alpha + \beta$ the gains of the omni-antenna and the array are comparable, resulting in a large reduction in gain in the composite antenna pattern.

By choosing a suitable inclination angle, an effective array height (h), and dipole parameters (L, W, S), a significant improvement in gain can be achieved in an angular region about $\theta = \alpha$. Appreciable improvement in antenna sidelobe level can also be realized. These improvements are achieved at the expense of a relatively small loss in gain over a region where the gain of the omni-antenna is relatively high. The beam shaping structure can be used without modification to shape right hand and left hand circularly polarized and linearly polarized low gain antennas.

At $\theta = \alpha$, the direct and reflected signals are in phase. If the frequency of operation is increased, the phase of the reflected signal will lag the phase of the direct signal. Conversely, if the frequency is decreased, the phase of the reflected signal will lead the phase of the direct signal. A change in phase between the direct and reflected signal will result in a loss of gain at $\theta = \alpha$. If the direct and reflected signals are equal in magnitude, a 40° relative phase change corresponding to a 5% change in frequency over a path length of 2λ will result in a loss of gain of 1 dB.

Provided the dipoles are less than $\lambda/4$ at the highest frequency of operation, there will be no change in phase due to the dipoles as the frequency is changed. However, the magnitude of the dipole reflection coefficient increases with frequency and must be taken into account when estimating gain.

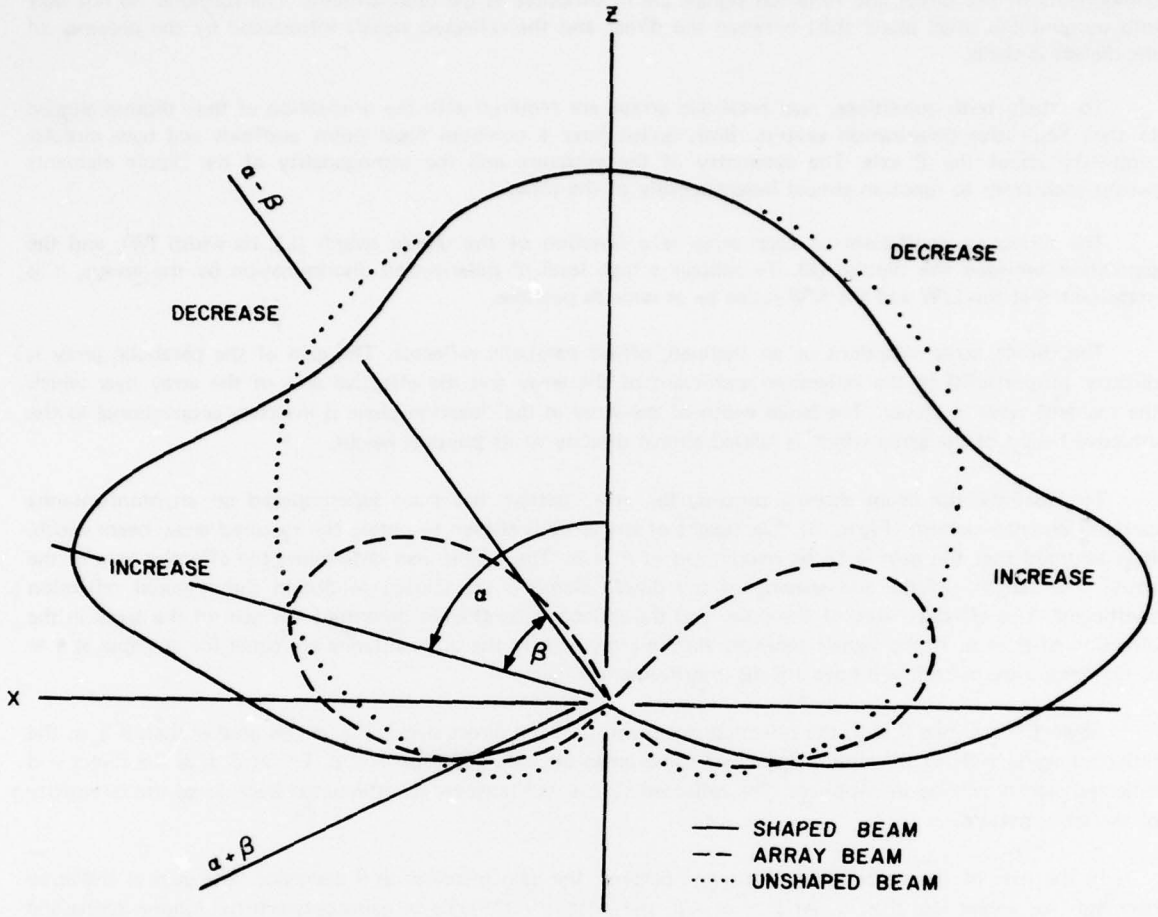

Figure 3. Beamshaping Process

There is no general formula for computing bandwidth. Each shaped beam antenna will have a different bandwidth depending on its gain and sidelobe requirements. It is evident that the technique can be used to shape the antenna pattern at only one of the NAVSTAR frequencies, in this case 1575 MHz. The omni-directional antenna pattern is essentially unshaped at the lower NAVSTAR frequency.

4.3 MEASUREMENTS

A number of selected antenna patterns, measured at the same azimuth angle, is contained in Appendix A. A complete data package which includes unshaped antenna patterns and patterns measured at a number of azimuth angles may be obtained from the author.

The antenna has a shaped beam between 1515 MHz and 1635 MHz. (Appendix A, patterns 27, 35, 43, 51, 59, 67 and 75). Over the operational bandwidth of 1555 MHz to 1595 MHz, a nominal 0 dbi circularly polarized gain is obtained between zenith and 7° above the horizon. The antenna has a maximum ellipticity ratio of 4.5 dB, a gain slope of 0.5 dB/degree in the vicinity of the horizon, and a maximum sidelobe level measured on a power basis of -18.0 dbi. The patterns are unshaped at the lower NAVSTAR frequencies (Appendix A, patterns 83, 87, and 91). The patterns are symmetrical about the Z axis and almost independent of azimuth angle.

There exists a trade-off between minimum gain, coverage requirements, gain slope and sidelobe level. By modifying slightly the omni-antenna configuration and its position above the ground plane, the minimum 0 dbi circularly polarized coverage can be extended at the expense of gain slope and sidelobe level (Appendix A, pattern 95). The 0 dbi minimum coverage can be extended to 2° above the horizon at the expense of a gain slope reduction in the vicinity of the horizon (0.3 dB/degree) and an increase in sidelobe level (−12 dbi). The patterns are again unshaped at the lower NAVSTAR frequencies (Appendix A, pattern 99).

Tests were carried out which showed that the antenna is insensitive to changes in ground plane size for diameters greater than 18".

A V.S.W.R. of less than 1.5 was measured between 1225 MHz and 1575 MHz. An external balun was used to feed the antenna. In an operational system, the balun would be made from microstrip and would be an integral part of the antenna.

4.4 MECHANICAL DESIGN

The antenna has an angle $\alpha = 75°$, a height of 12", a maximum diameter of 15", and sits on an 18" diameter ground plane. The shells are made of glass cloth and Emerson & Cuming Stycast 35DT, which has a dielectric constant of 2.2 and a specific gravity of 1.5. The dipole elements are made of 3M metallic tape. The elements have a length of 1.65", a width of 0.065" and a nominal transverse spacing of 0.6". They are staggered as shown on Plate 3. Tests have shown that copper adheres well to the dielectric material and that the dipole elements could be formed by a plating/photoetching process. No structural analysis has been carried out on the Antenna configuration.

5. MEASUREMENT ACCURACY

A rigorous statistical analysis has not been carried out to determine the statistical distribution on each source of measurement error. To simplify the analysis it is assumed that the statistical distribution of each source of error is Gaussian. A 2 σ error has been assigned to the principal sources of electrical error, based on manufacture data, facility calibration data and visual observation.

Anechoic chamber reflection error at 0 dbi	: 0.3 dB
Standard Gain Horn Calibration	: 0.2 dB
Signal Source Stability	: 0.3 dB
Receiver Stability	0.2 dB
Recorder Repeatability	0.2 dB
Attenuator Error	0.2 dB
Connector Mismatch	0.1 dB

Finding the square root of the sum of the squares of the above errors gives a total 2 σ error of 0.55 dB, i.e. there is a 95% probability that the calibration lines on the antenna patterns do not differ from the true gain value by more than 0.55 dB.

The ellipticity ratio at any angle within the desired coverage is estimated to have a 2 σ error of 0.5 dB. It is estimated that the 2 σ absolute angular error is 2° and the 2 σ relative angular error, 1°.

6. SUMMARY AND CONCLUSIONS

Two new types of shaped beam antennas have been designed and developed at CRC for DND.

The Hybrid Spiral Antenna is a compact antenna which has an instantaneous bandwidth of the order of 25%. It provides a minimum circularly polarized gain of 0 dbi between zenith and a lower angular limit which varies from 10° above the horizon at 1575 MHz, to 18° above the horizon at 1225 MHz. The maximum ellipticity ratio within the required angular coverage varies from 5 dB at 1575 MHz to 7 dB at 1225 MHz. The patterns are symmetrical about the Z axis and almost independent of azimuth angle. The results are summarized in Table 2.

The Composite Array Antenna provides a shaped antenna beam over an instantaneous bandwidth of 5% at 1575 MHz. The antenna pattern is unshaped at 1225 MHz. A minimum circularly polarized gain of 0 dbi is obtained between zenith and a lower angular limit which is determined by the permissible sidelobe levels. The lower limit can vary from 7° above the horizon with a sidelobe level measured on a power basis of -18 dbi, to 2° above the horizon with a sidelobe level of -12 dbi. The results are summarized in Tables 3 and 4 respectively. The maximum ellipticity ratio is 4.5 dB within the required angular coverage. The antenna patterns are almost independent of ground plane size, are symmetrical about the Z axis and almost independent of azimuth angle.

Because of its size the antenna appears to be most suitable for land and sea applications. Although jamming has not been discussed in this report, the antenna appears to have some anti-jam capability. The antenna has a rapid change in gain versus angle in the vicinity of the horizon, of the order of 0.5 dB/degree. By tilting the antenna away from the jammer a significant reduction in jamming signal level could be achieved without an appreciable loss of angular coverage. This antenna is more complex than the Hybrid Spiral and further structural analysis is required to meet the environmental requirements and reduce the cost of production.

TABLE 2

Hybrid Spiral Antenna Performance

Frequency	Upper NAVSTAR Frequencies 1575 MHz		Lower NAVSTAR Frequencies 1225 MHz	
Angle θ (degrees)	Circularly Polarized Gain (dbi)	Ellipticity Ratio (db)	Circularly Polarized Gain (dbi)	Ellipticity Ratio (db)
0	3.5	1.5	0.0	3.5
10	3.5	2.0	1.75	1.5
20	3.5	2.0	0.5	5.5
30	3.0	4.0	0.5	4.0
40	1.75	3.5	0.0	6.0
50	1.0	3.5	0.0	5.5
60	0.5	2.5	1.0	2.0
70	2.0	4.5	0.25	2.0
80	0	5.0	-3.5	2.5
90	-4.5	7.0	-8.0	5.0

TABLE 3

Composite Array Antenna Performance: Sidelobe Level – 18 dbi

Frequency	Upper NAVSTAR Frequencies 1575 MHz		Lower NAVSTAR Frequencies 1225 MHz	
Angle θ (degrees)	Circularly Polarized Gain (dbi)	Ellipticity Ratio (db)	Circularly Polarized Gain (dbi)	Ellipticity Radio (db)
0	5.5	0.75	1.5	3.0
10	5.5	2.0	1.0	3.5
20	5.0	4.0	0.0	4.0
30	4.0	3.5	0.5	3.0
40	2.5	2.0	1.5	1.0
50	0.25	3.0	1.0	3.5
60	1.5	1.0	-1.0	7.5
70	2.5	0.75	-3.0	13.0
80	1.0	2.0	-4.5	14.0
90	-3.5	3.0	-5.0	16.5

TABLE 4

Composite Array Antenna Performance: Sidelobe Level – 12 dbi

Frequency	Upper NAVSTAR Frequencies 1575 MHz		Lower NAVSTAR Frequencies 1225 MHz	
Angle θ (degrees)	Circularly Polarized Gain (dbi)	Ellipticity Ratio (db)	Circularly Polarized Gain (dbi)	Ellipticity Ratio (db)
0	2.5	2.0	4.0	3.0
10	2.0	2.0	3.5	3.0
20	2.5	2.5	2.5	5.0
30	2.5	3.0	1.5	6.5
40	1.5	4.0	1.0	7.0
50	0.0	3.5	0.0	8.0
60	0.5	3.0	-2.75	9.0
70	1.75	3.5	-6.0	12.0
80	1.00	3.0	-8.0	>20.0
90	-1.00	3.5		

7. ACKNOWLEDGEMENTS

I would like to thank Mr. J. Charbonneau and his staff at the CRC Model Shop who were responsible for fabricating the antennas and Mr. J.G. Dumoulin who carried out some of the antenna measurements.

APPENDIX A

SELECTED ANTENNA PATTERNS

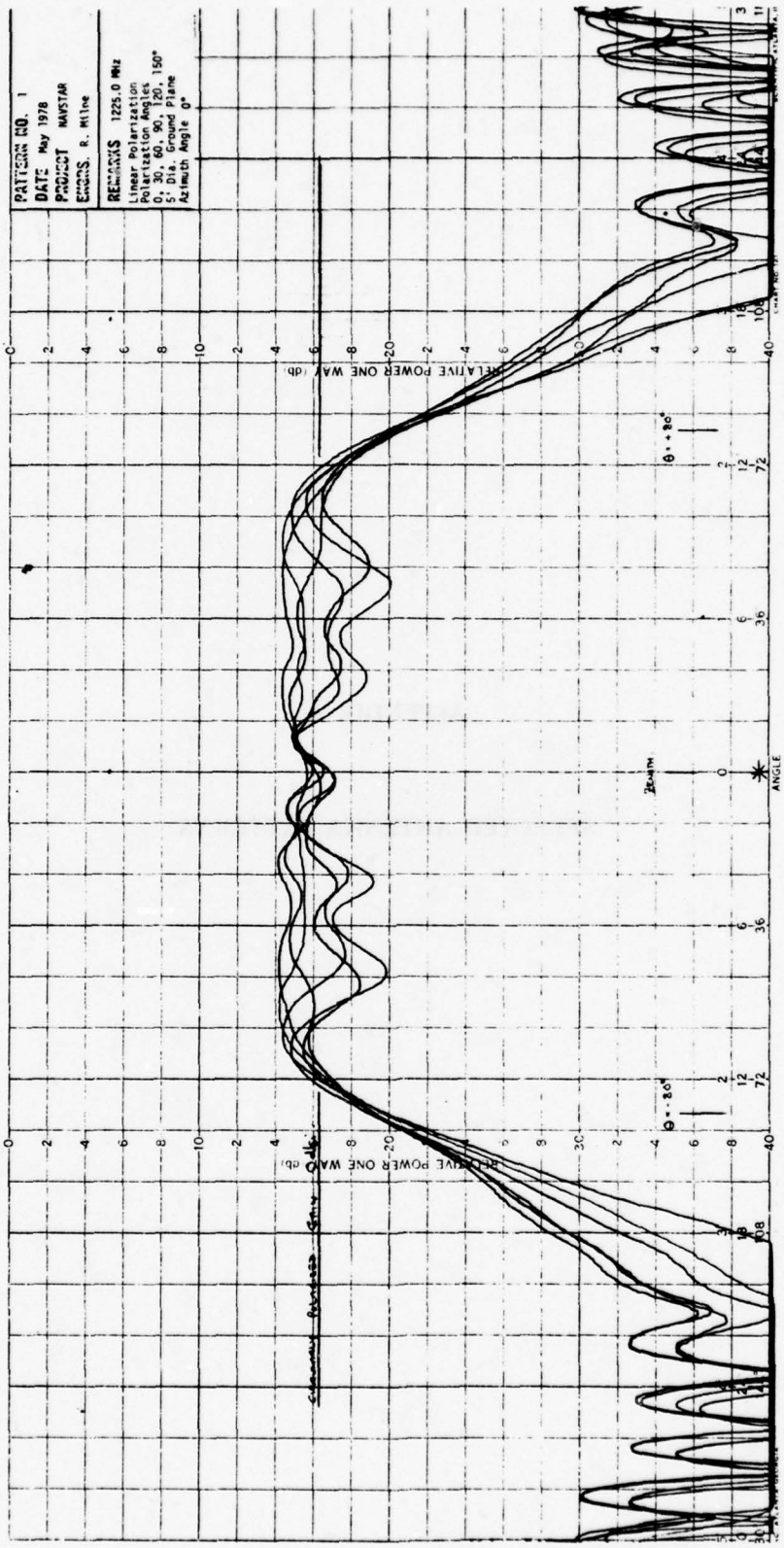

Figure A1. Antenna Pattern No. 1

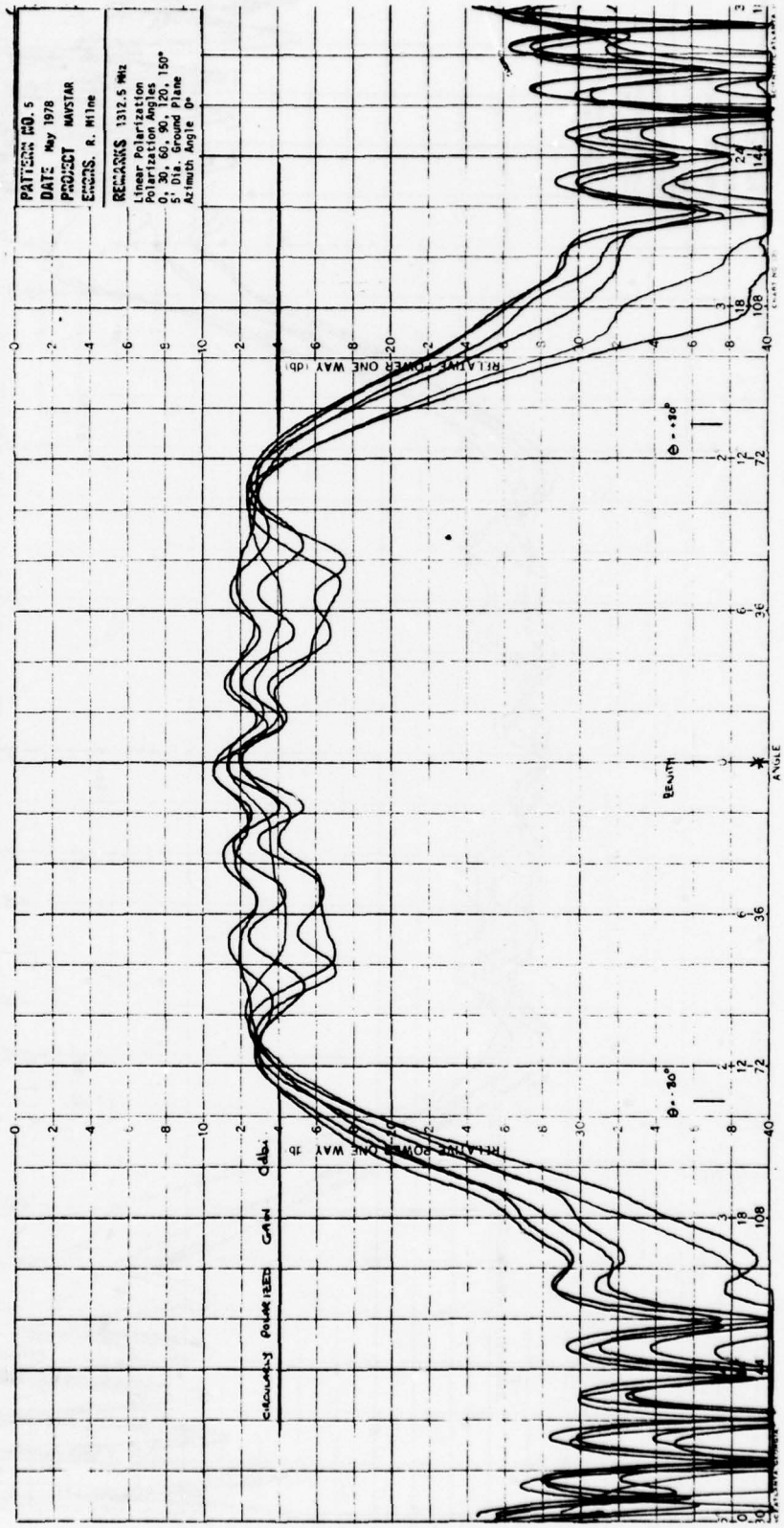

Figure A2. Antenna Pattern No. 5

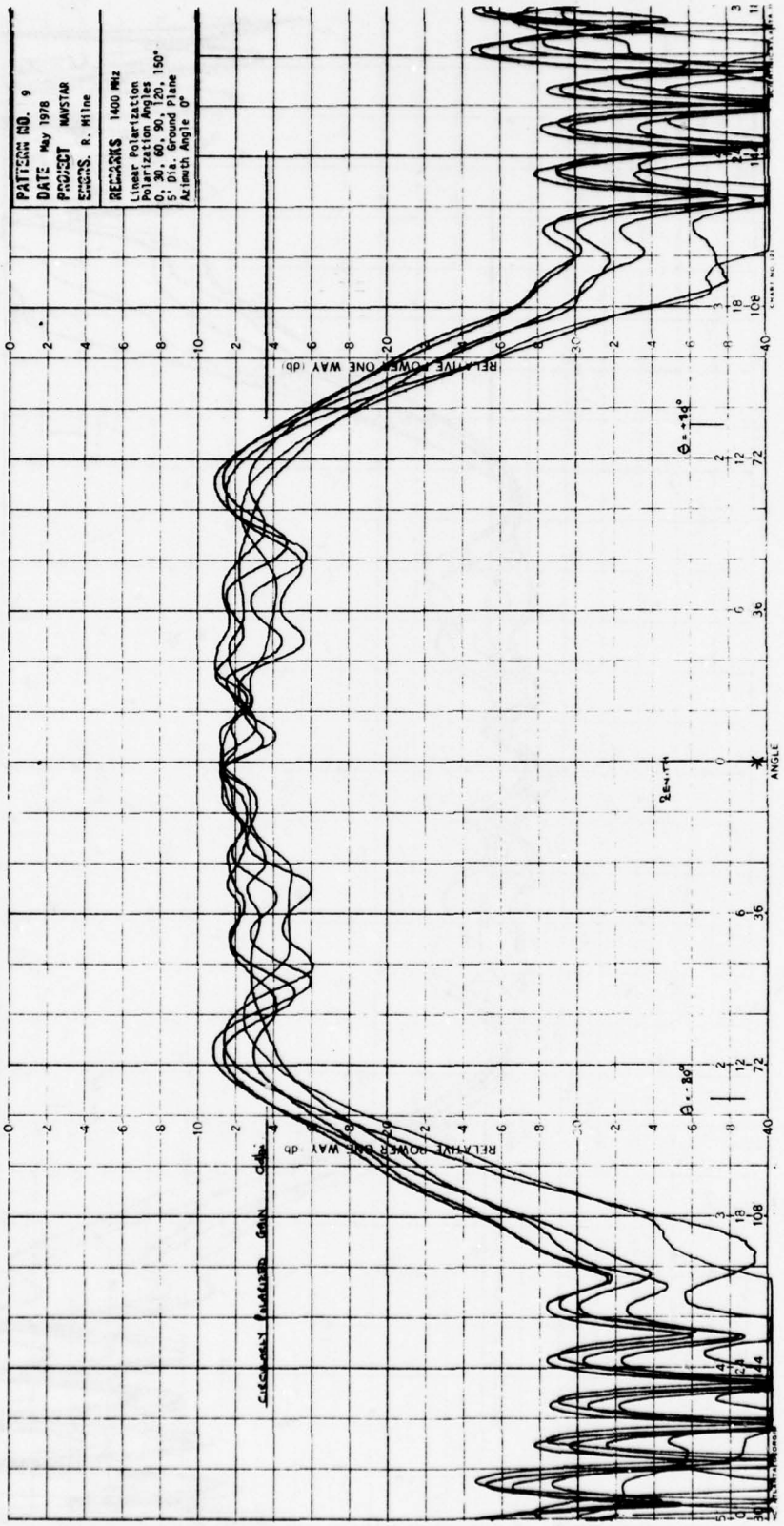

Figure A3. Antenna Pattern No. 9

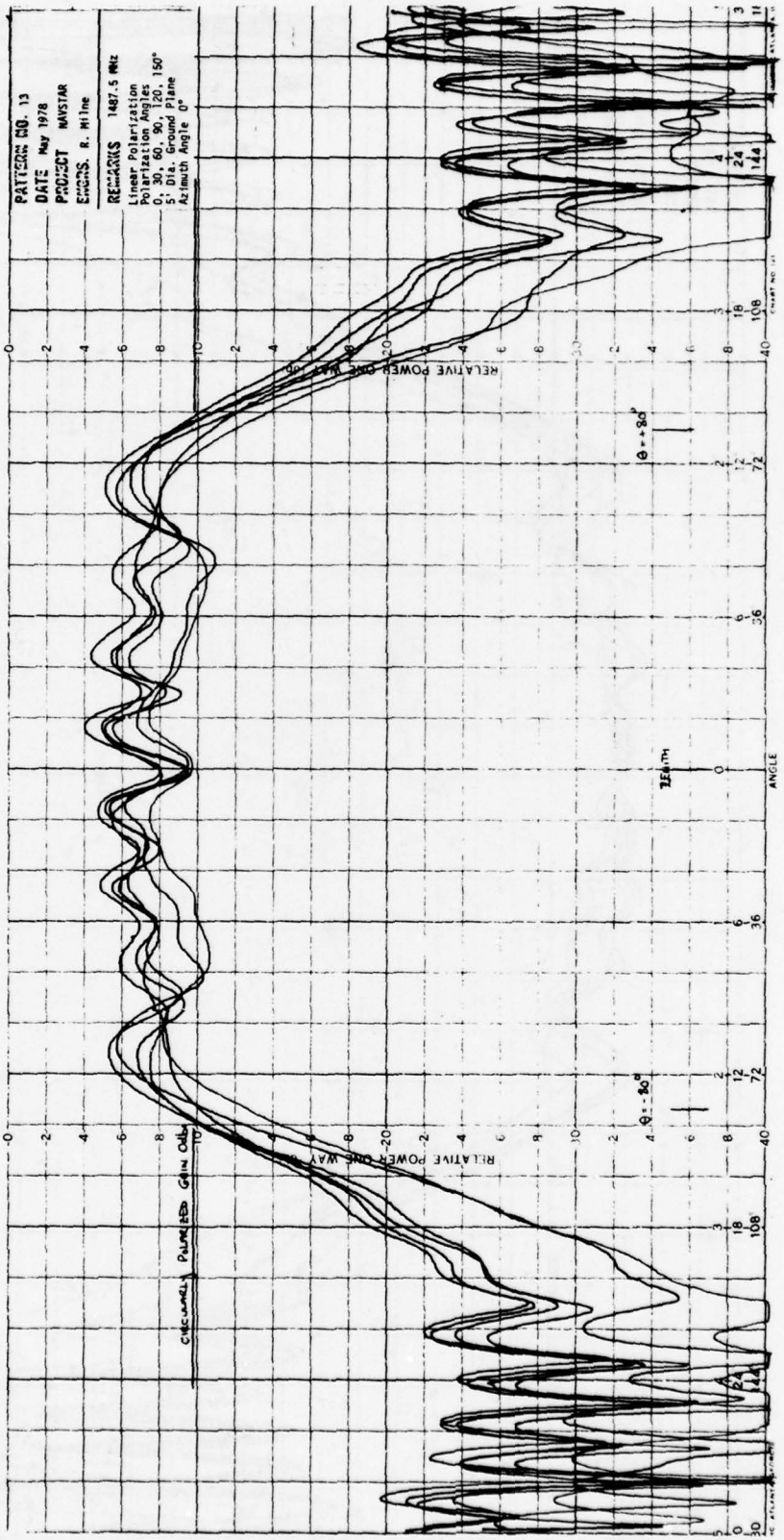

Figure A4. Antenna Pattern No. 13

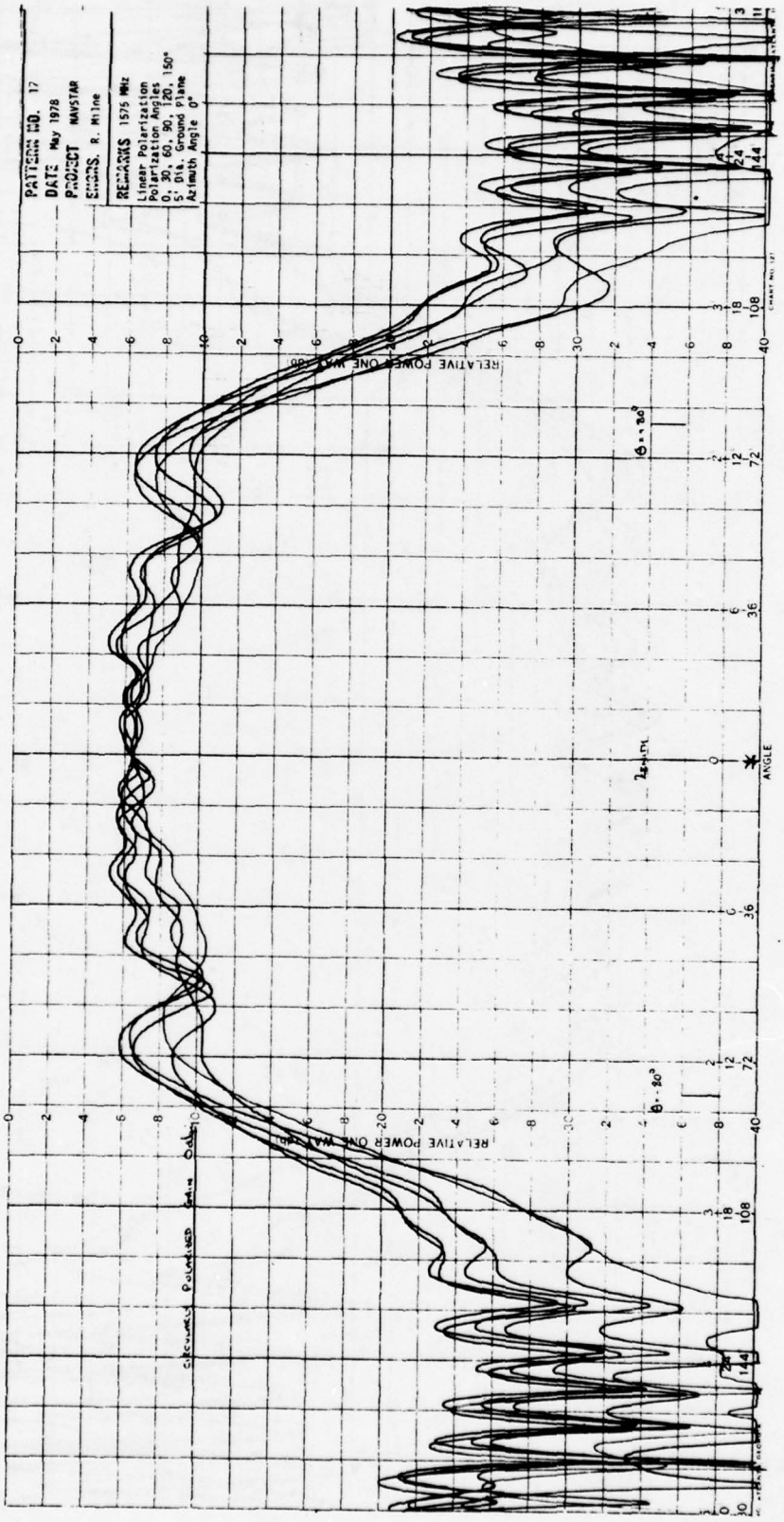

Figure A5. Antenna Pattern No. 17

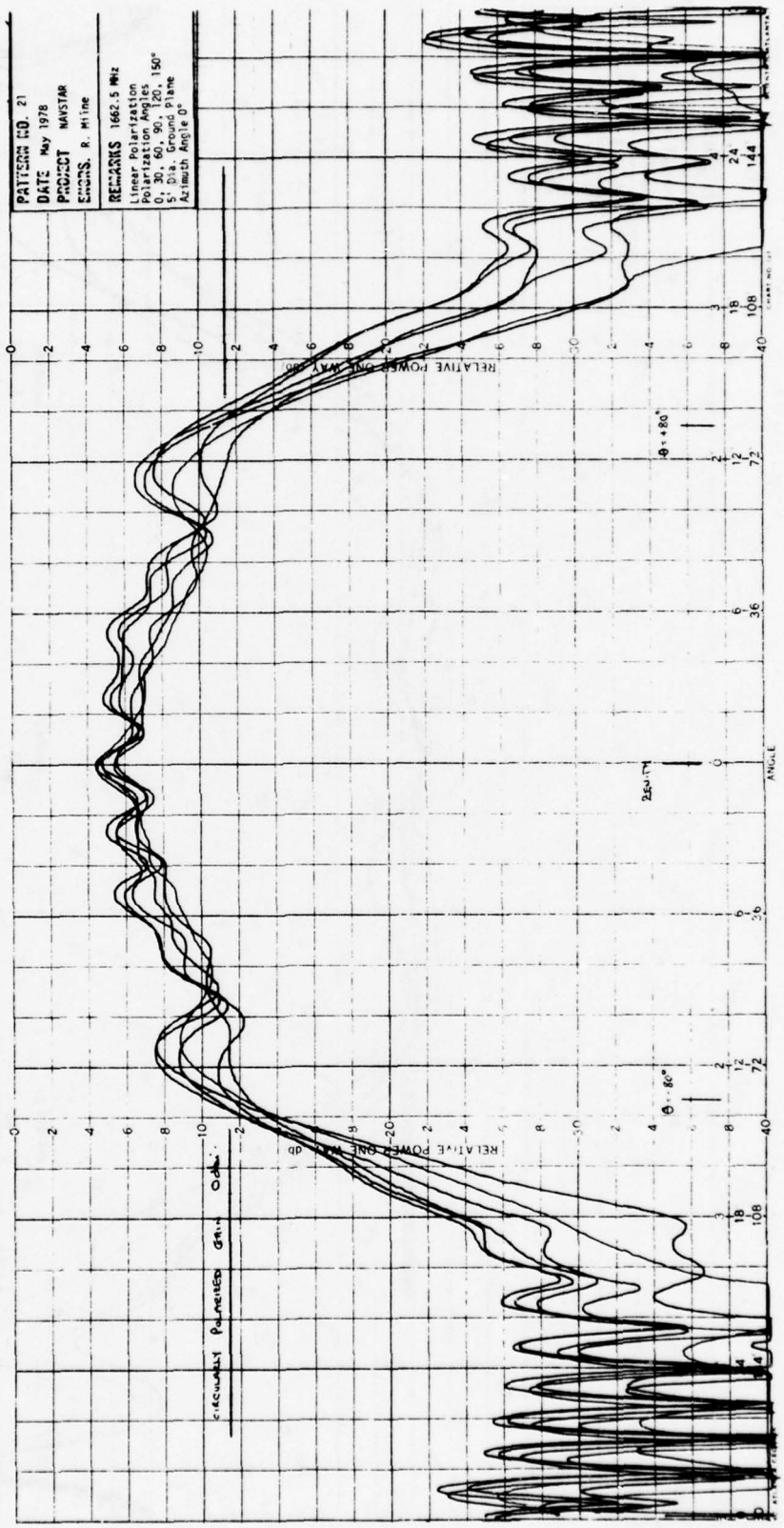

Figure A6. Antenna Pattern No. 21

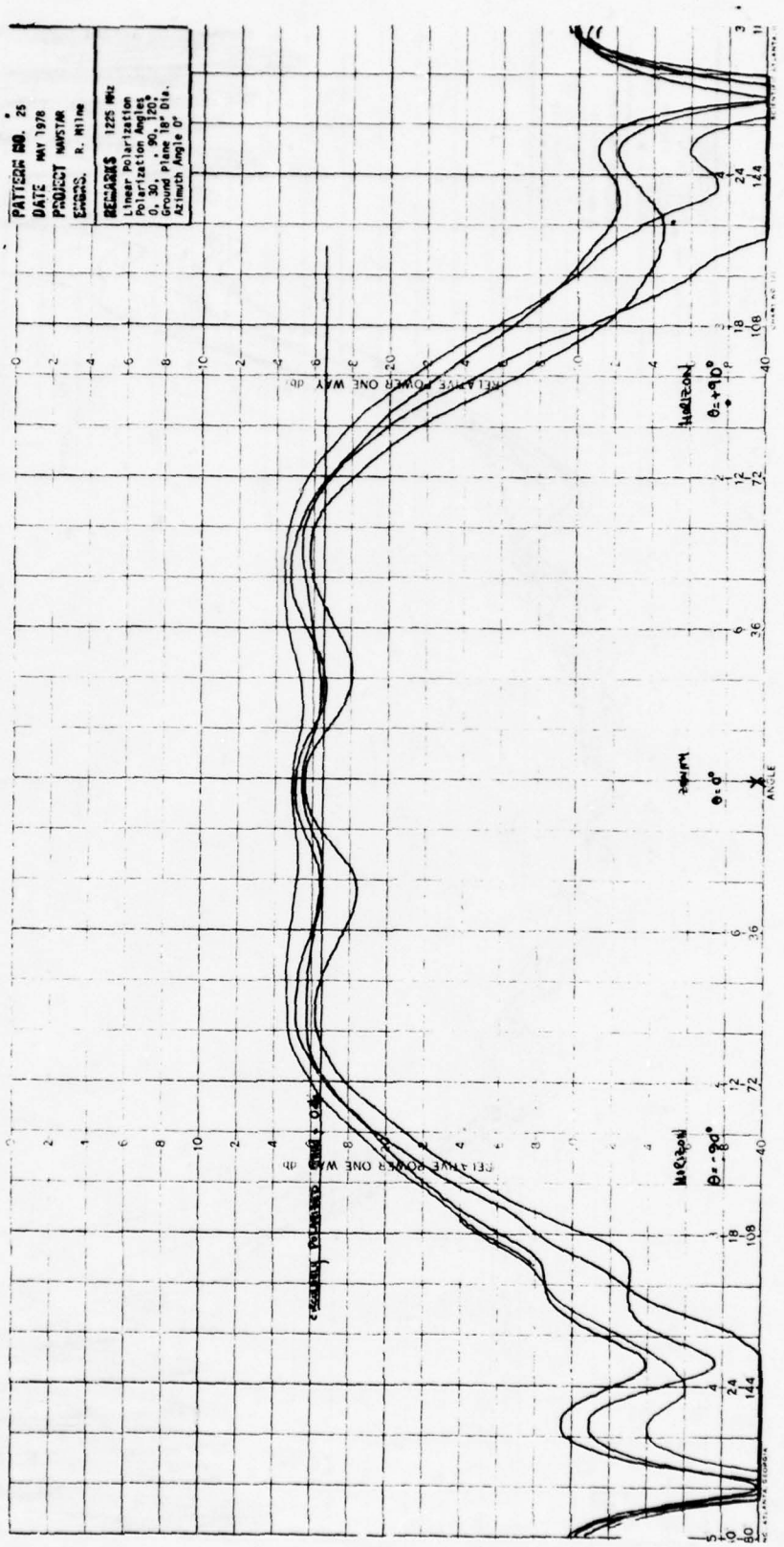

Figure A7. Antenna Pattern No. 25

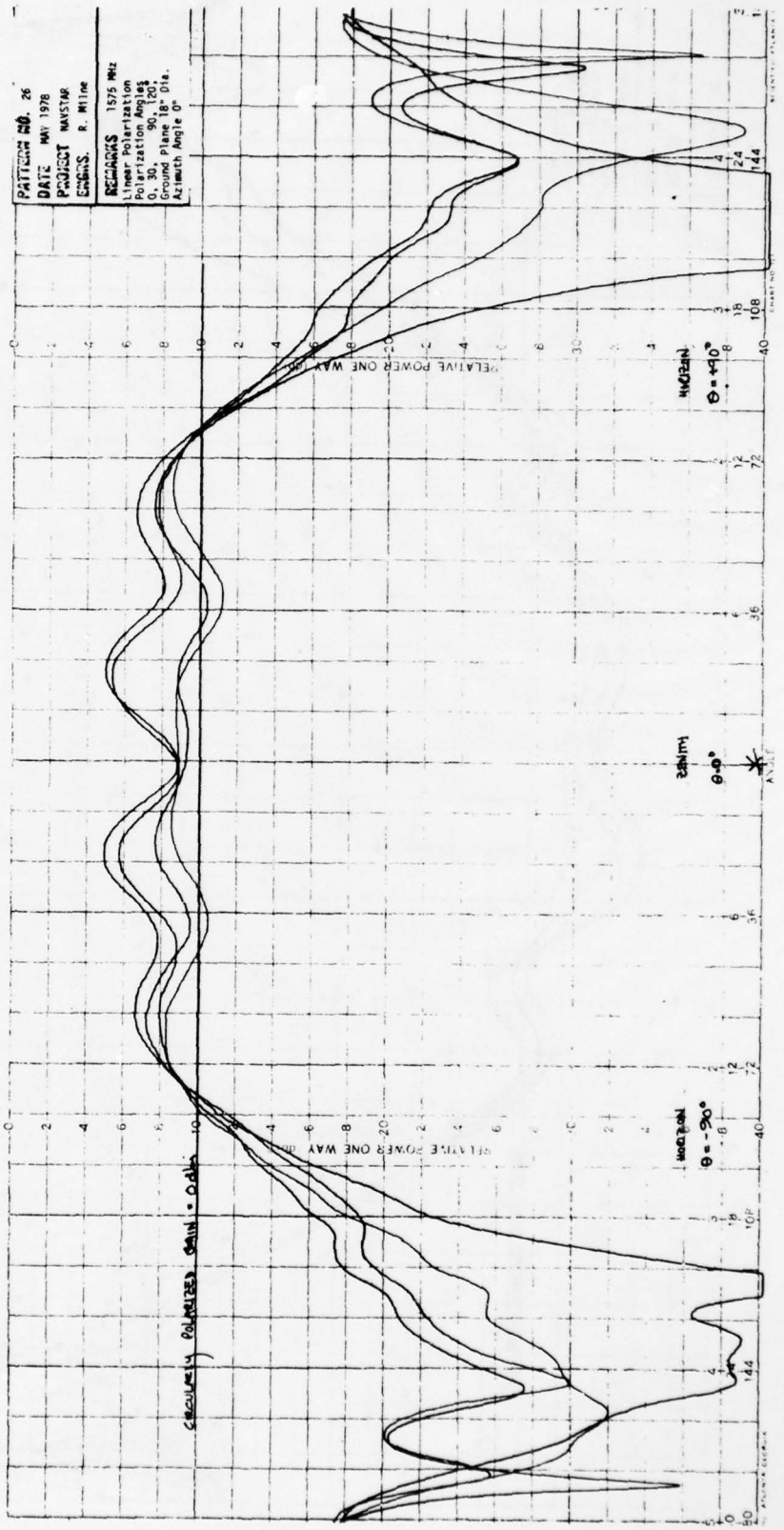

Figure A8. Antenna Pattern No. 26

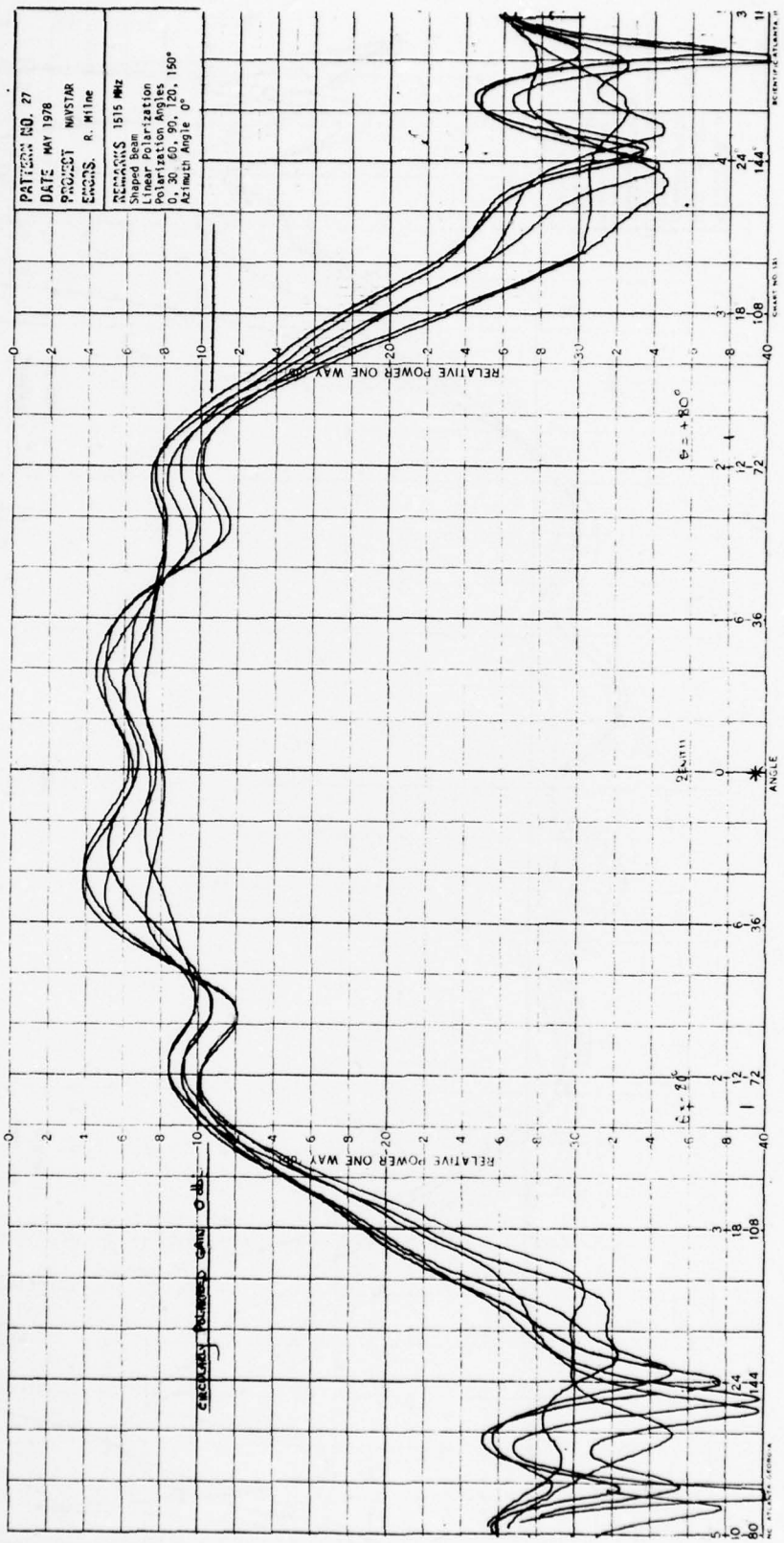

Figure A9. Antenna Pattern No. 27

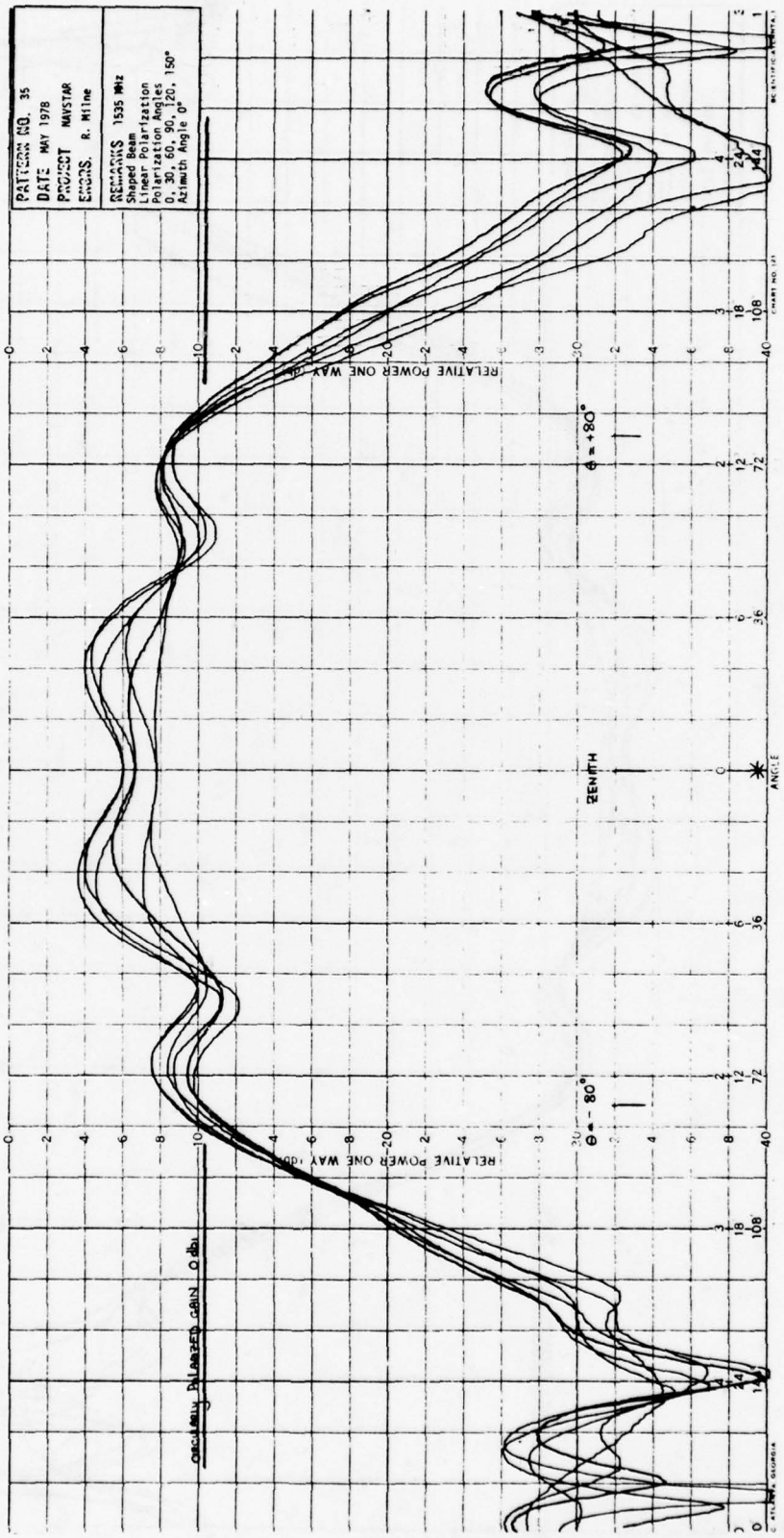

Figure A10. Antenna Pattern No. 35

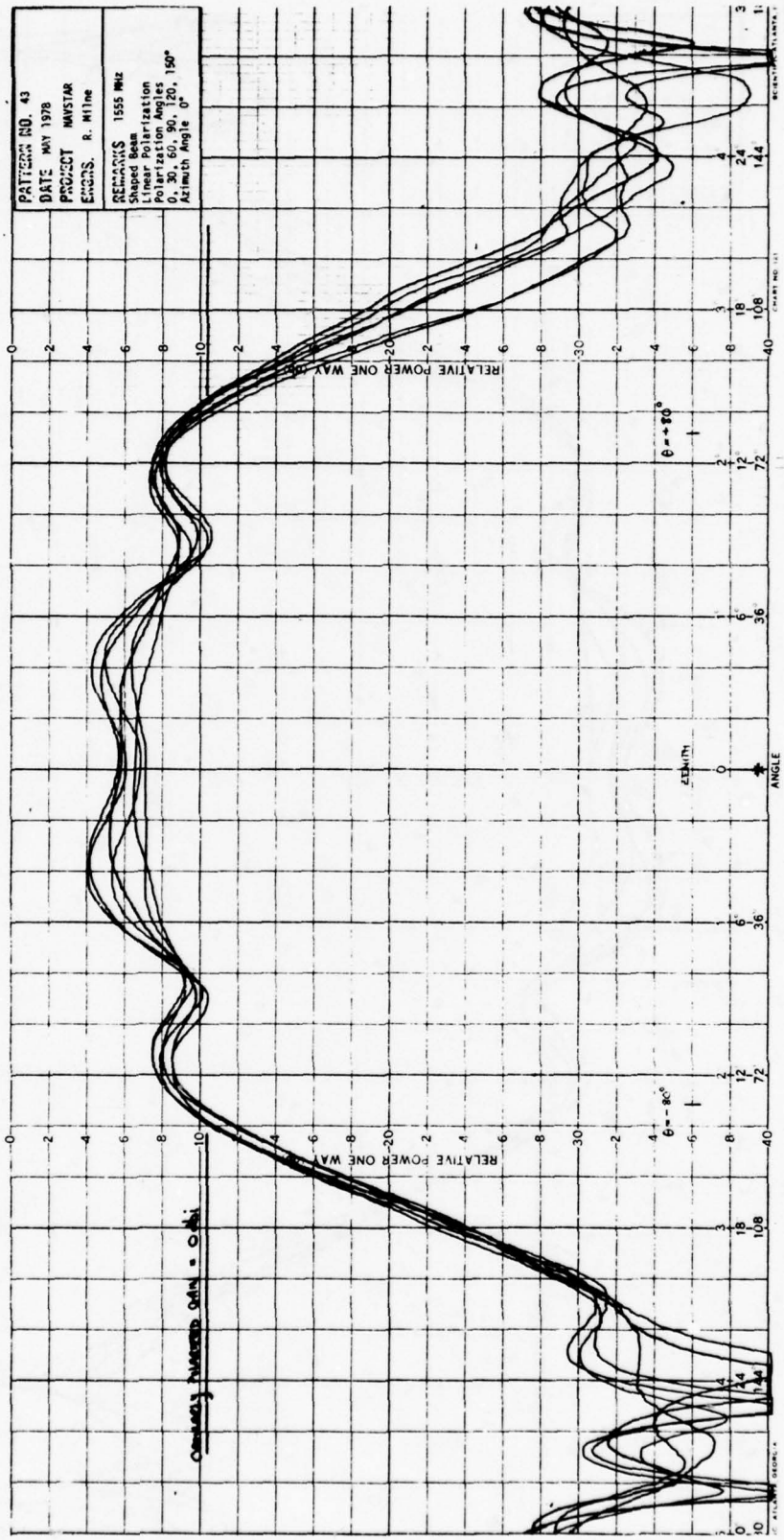

Figure A11. Antenna Pattern No. 43

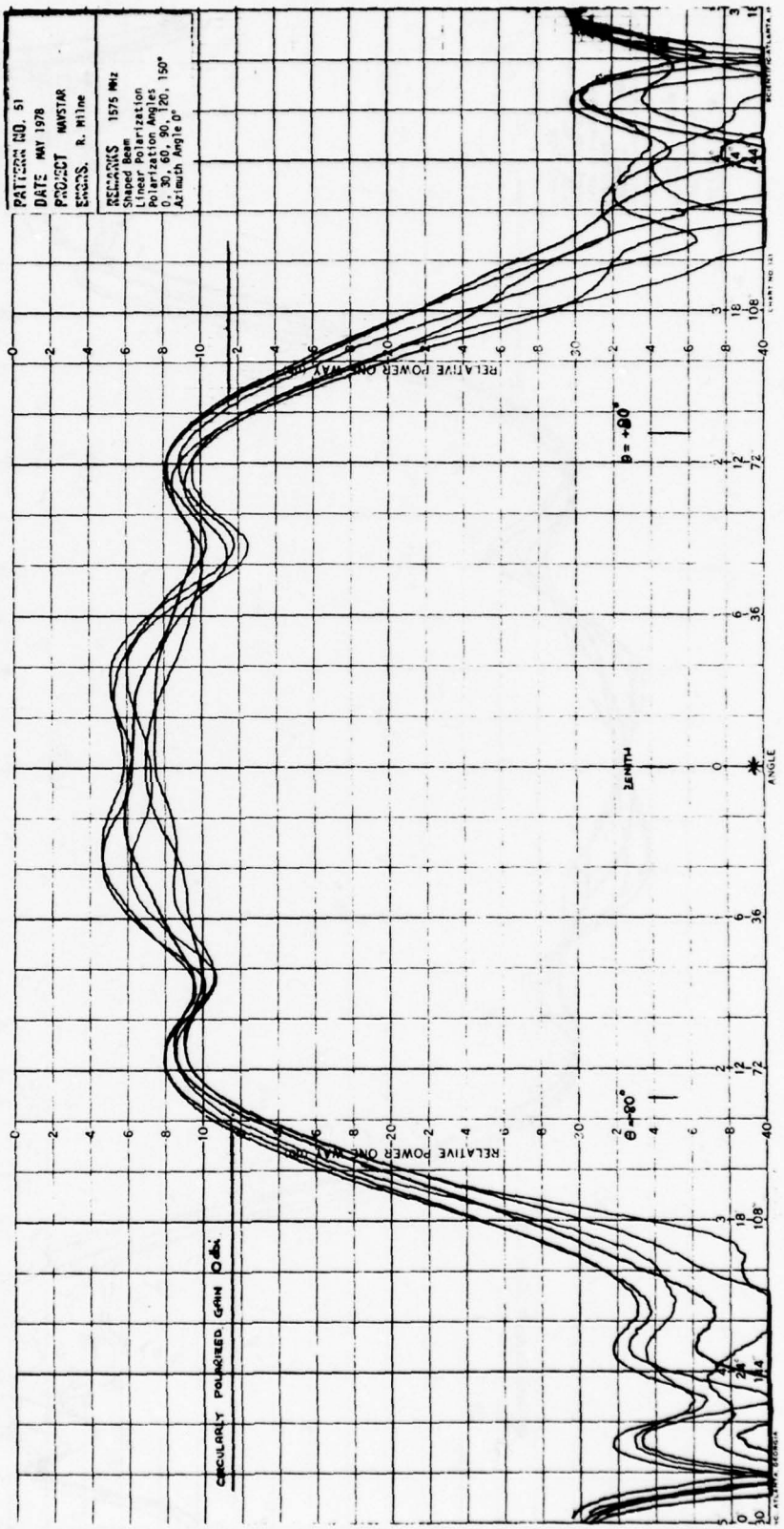

Figure A12. Antenna Pattern No. 51

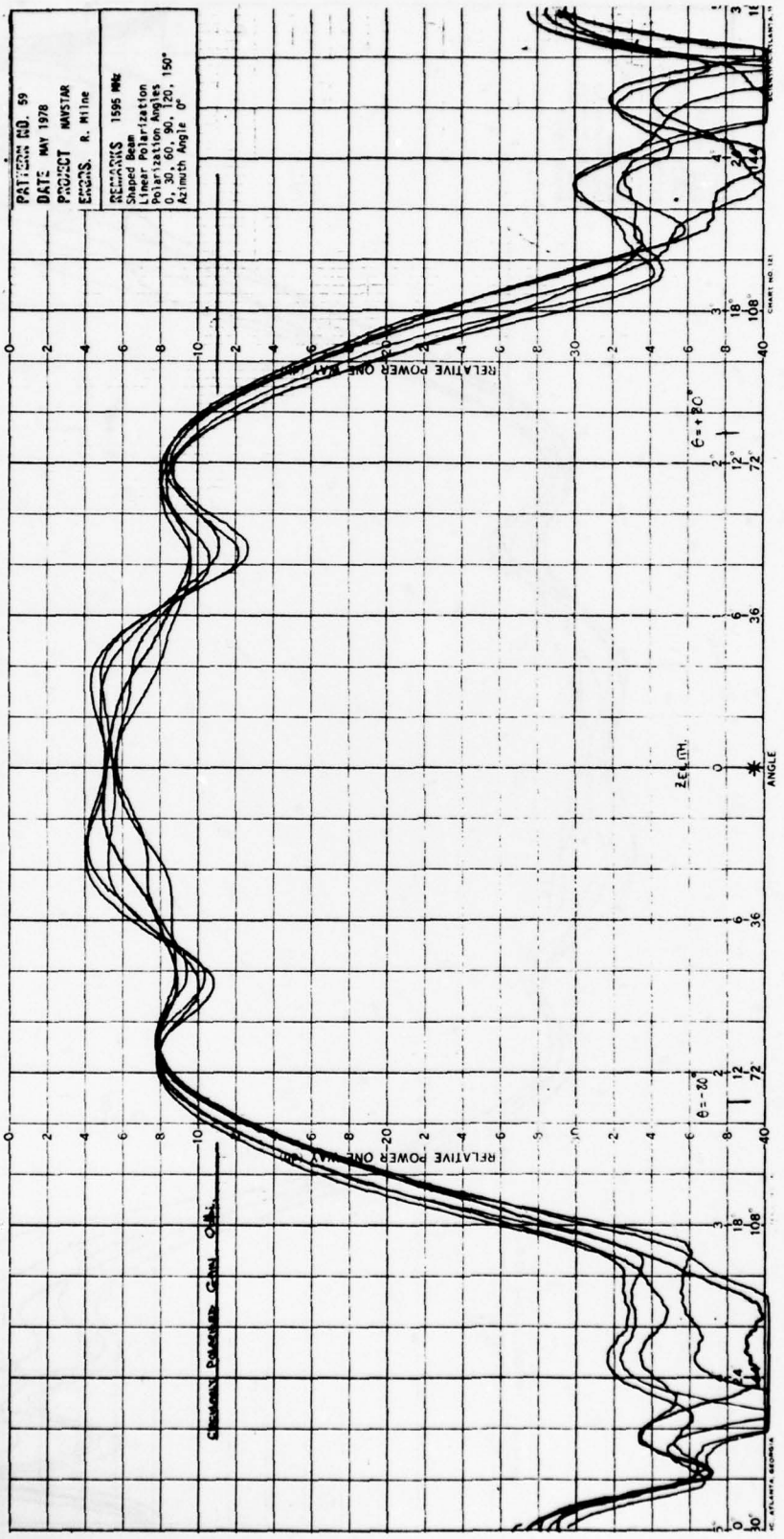

Figure A13. Antenna Pattern No. 59

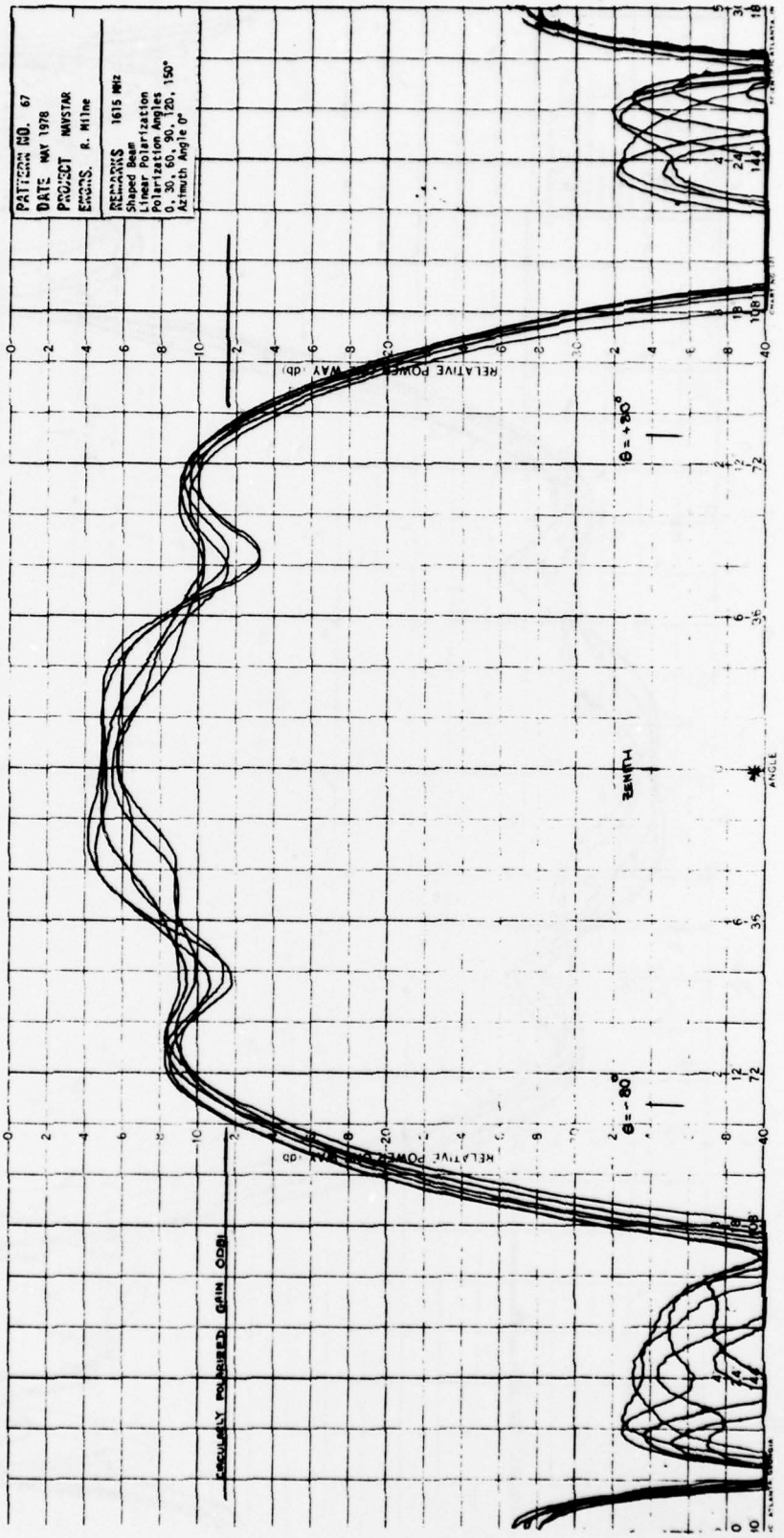

Figure A14. Antenna Pattern No. 67

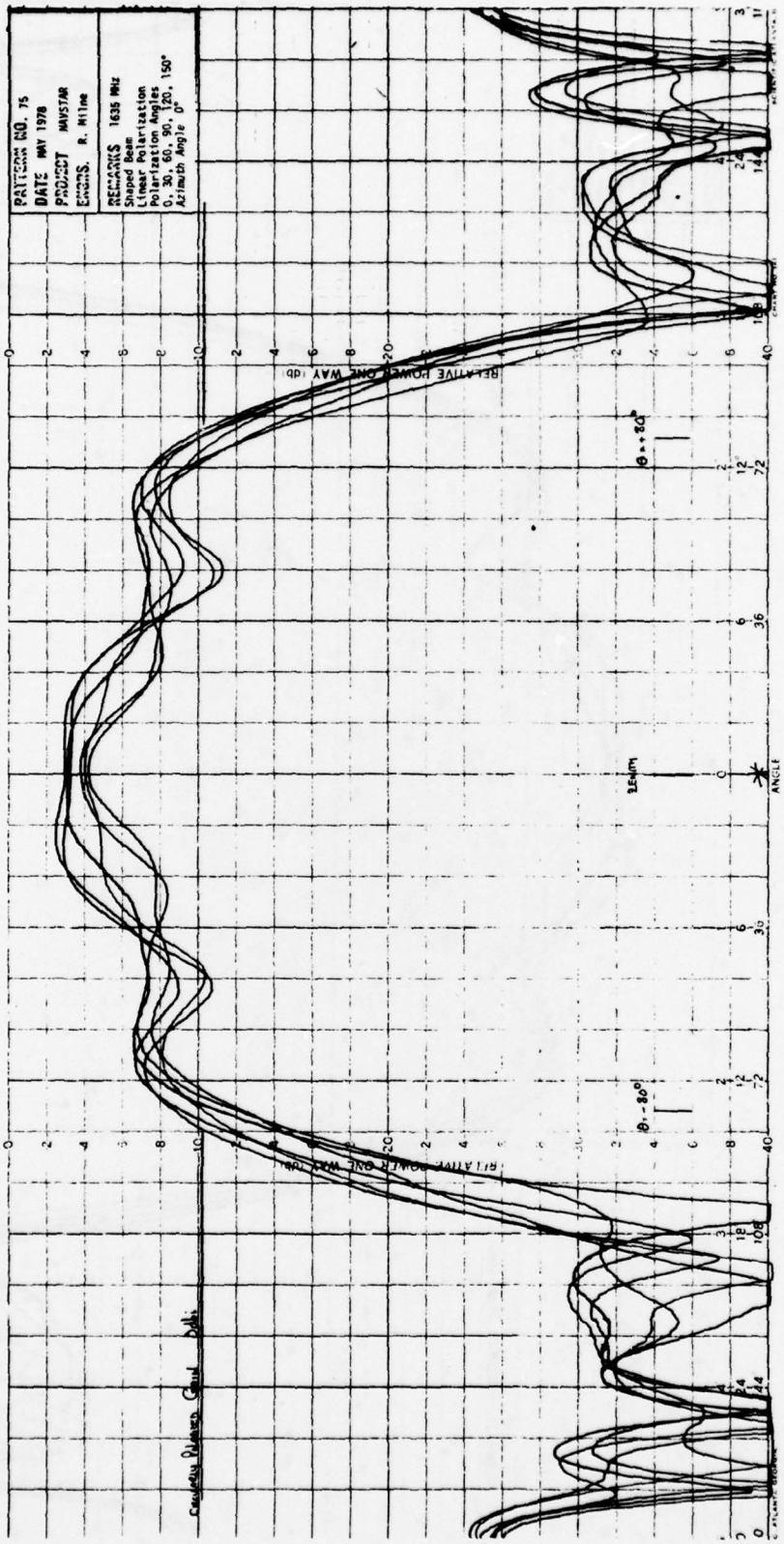

Figure A15. Antenna Pattern No. 75

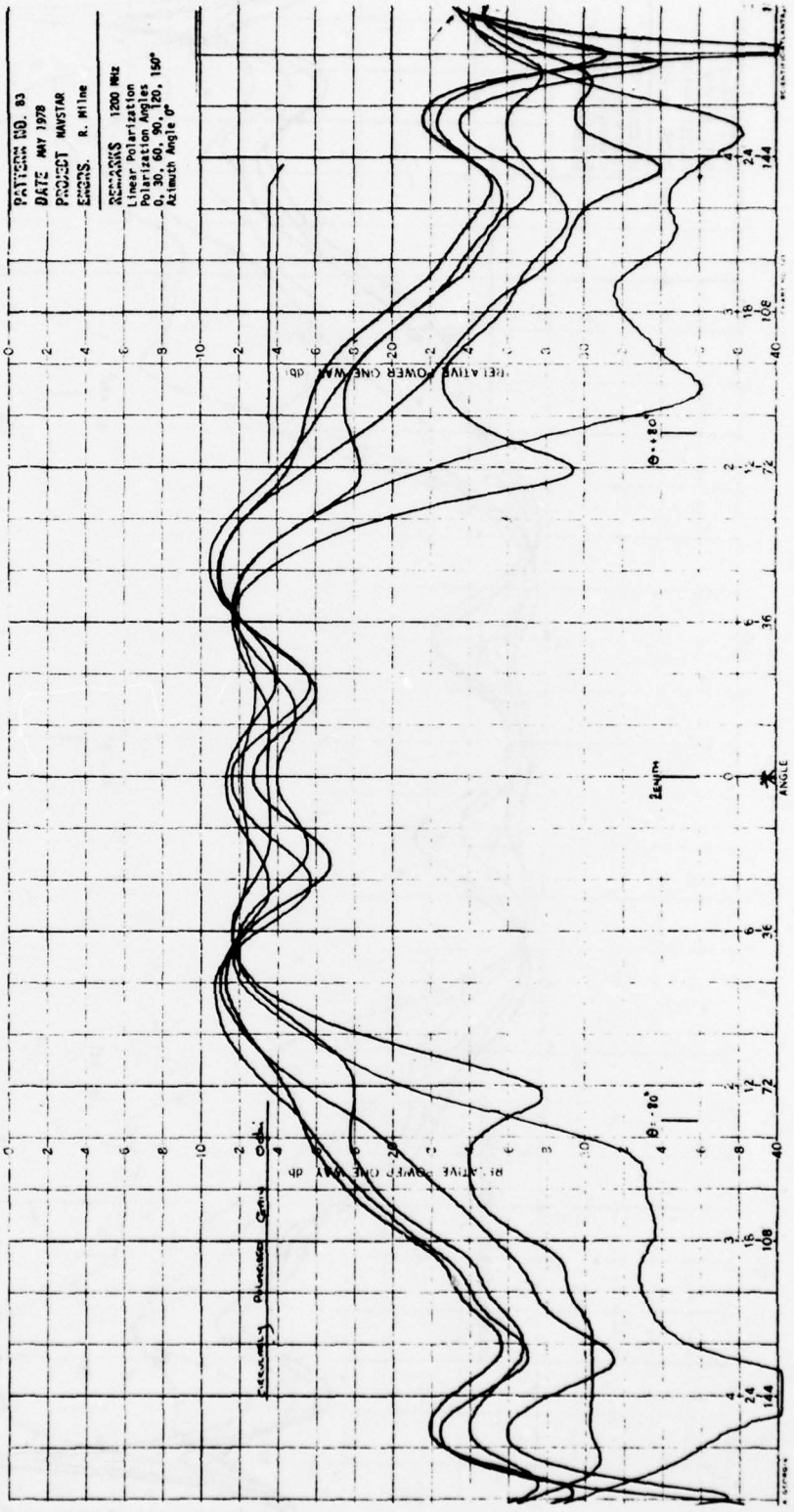

Figure A16. Antenna Pattern No. 83

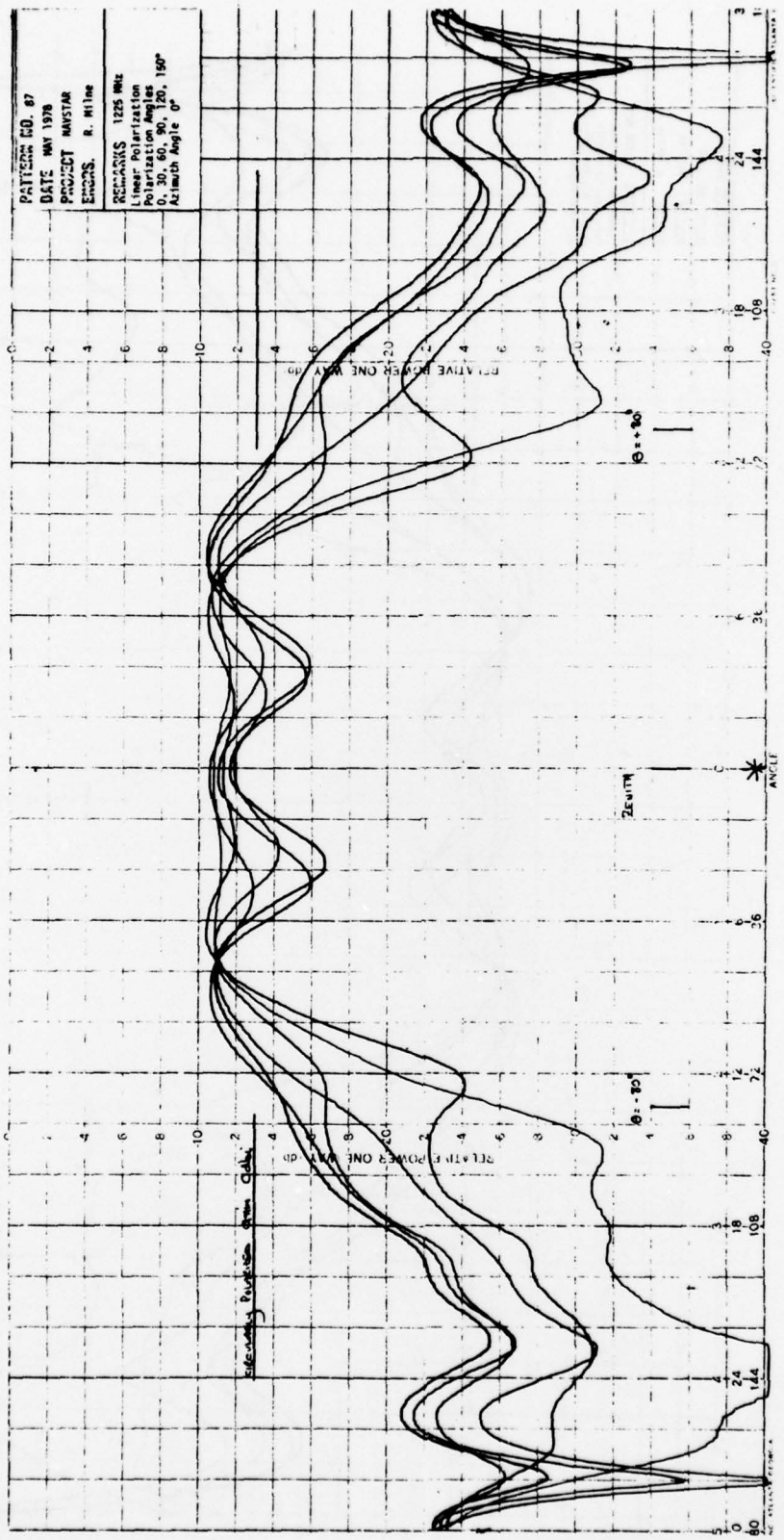

Figure A17. Antenna Pattern No. 87

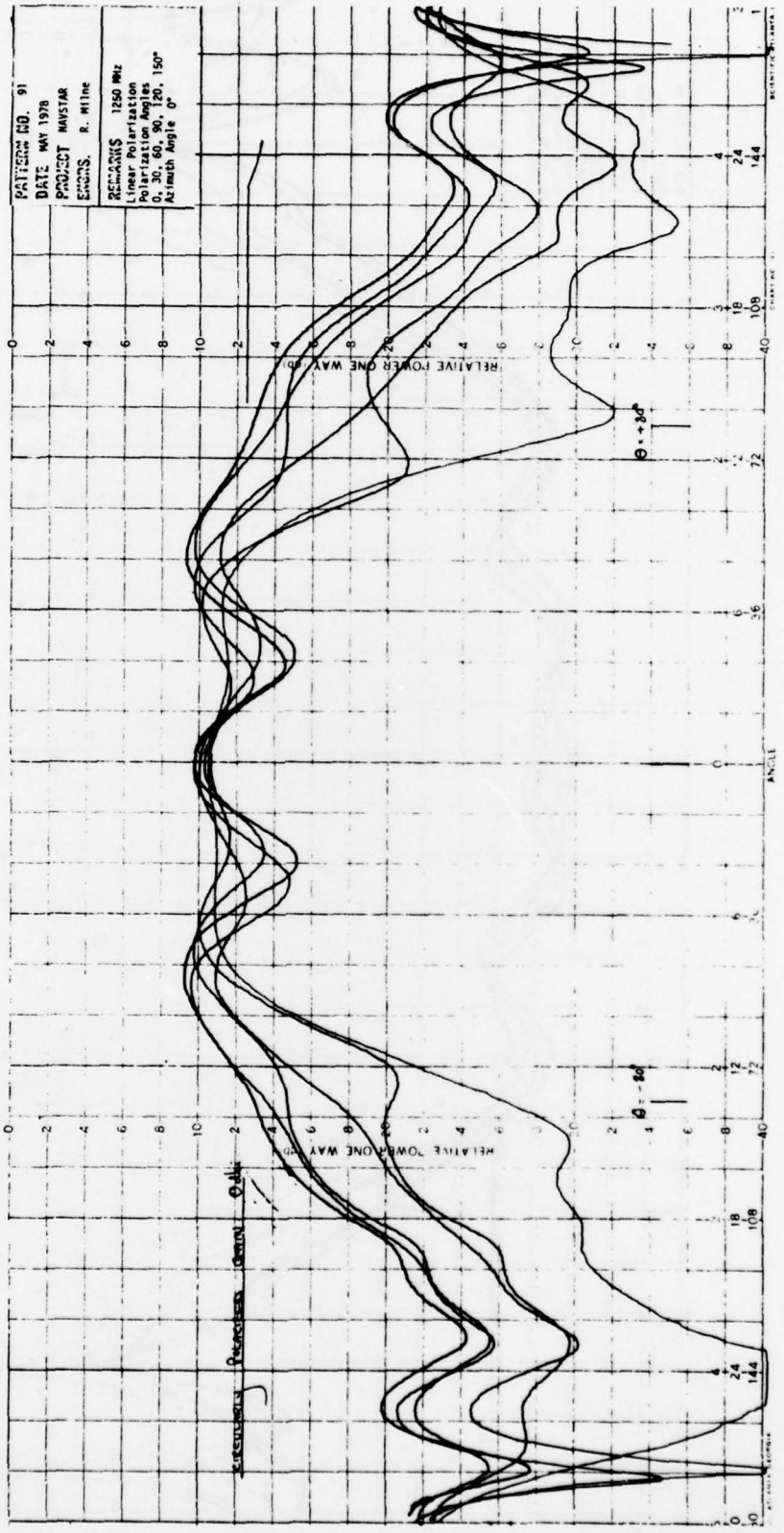

Figure A18. Antenna Pattern No. 91

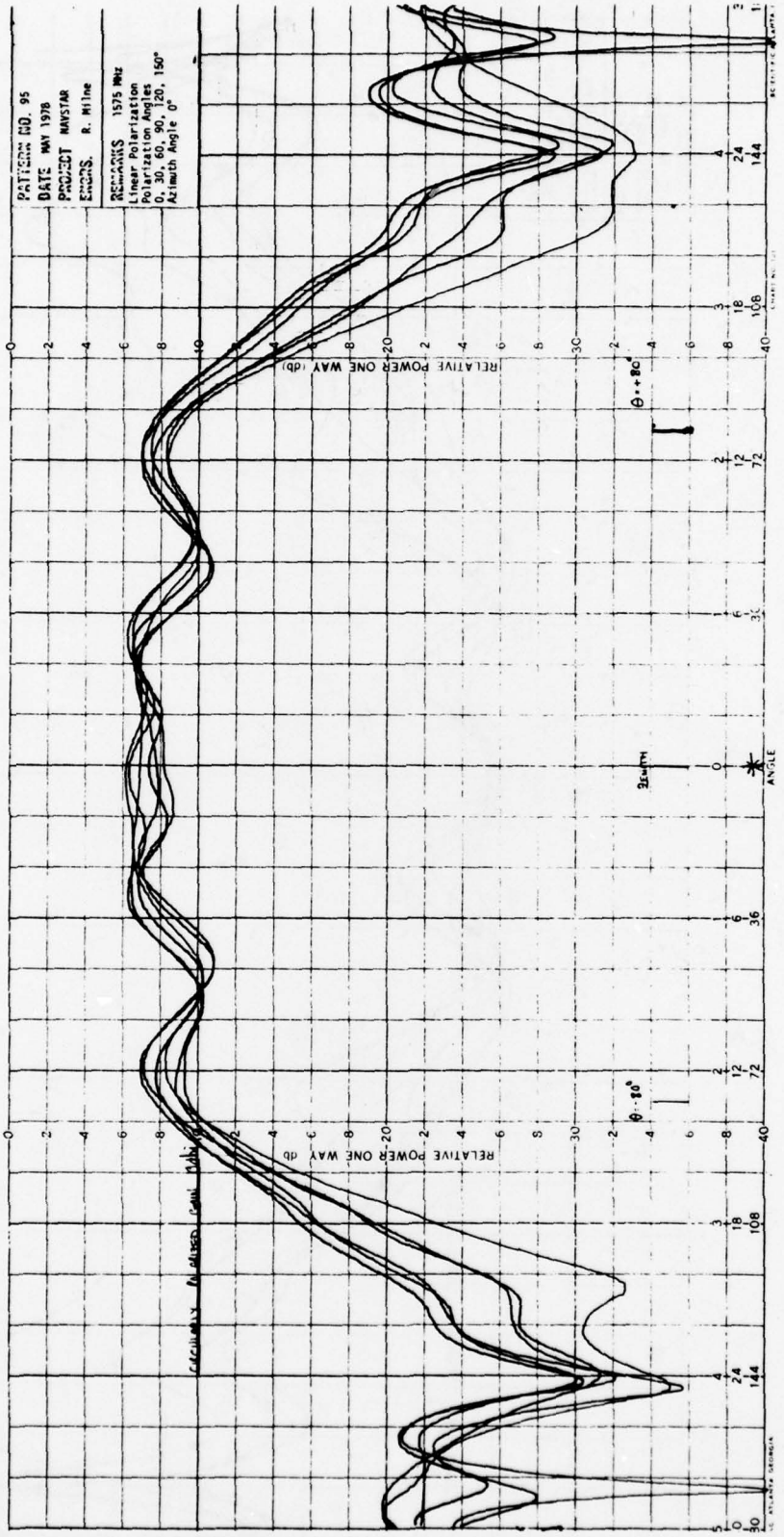

Figure A19. Antenna Pattern No. 95

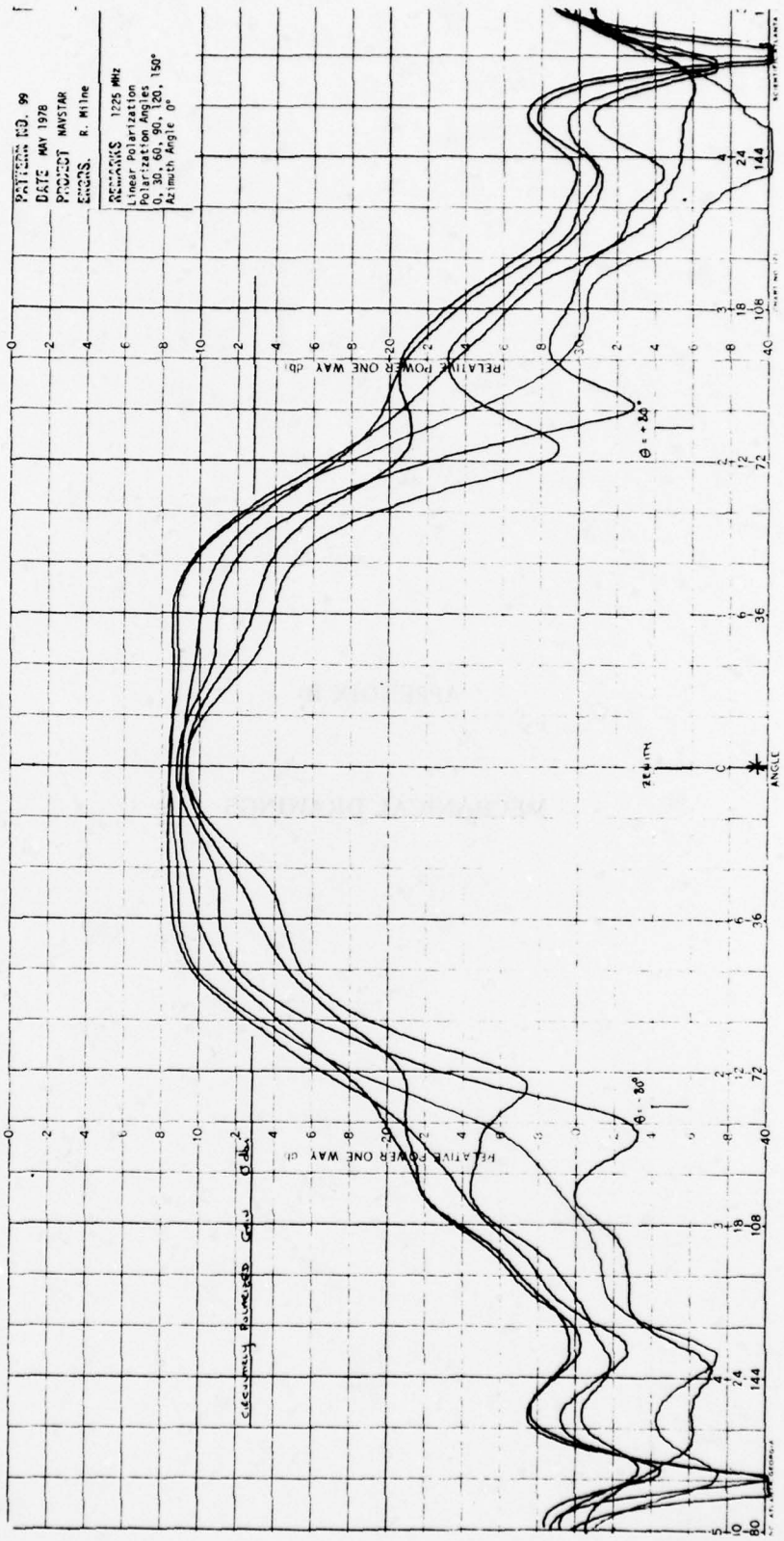

Figure A20. Antenna Pattern No. 99

APPENDIX B

MECHANICAL DRAWINGS

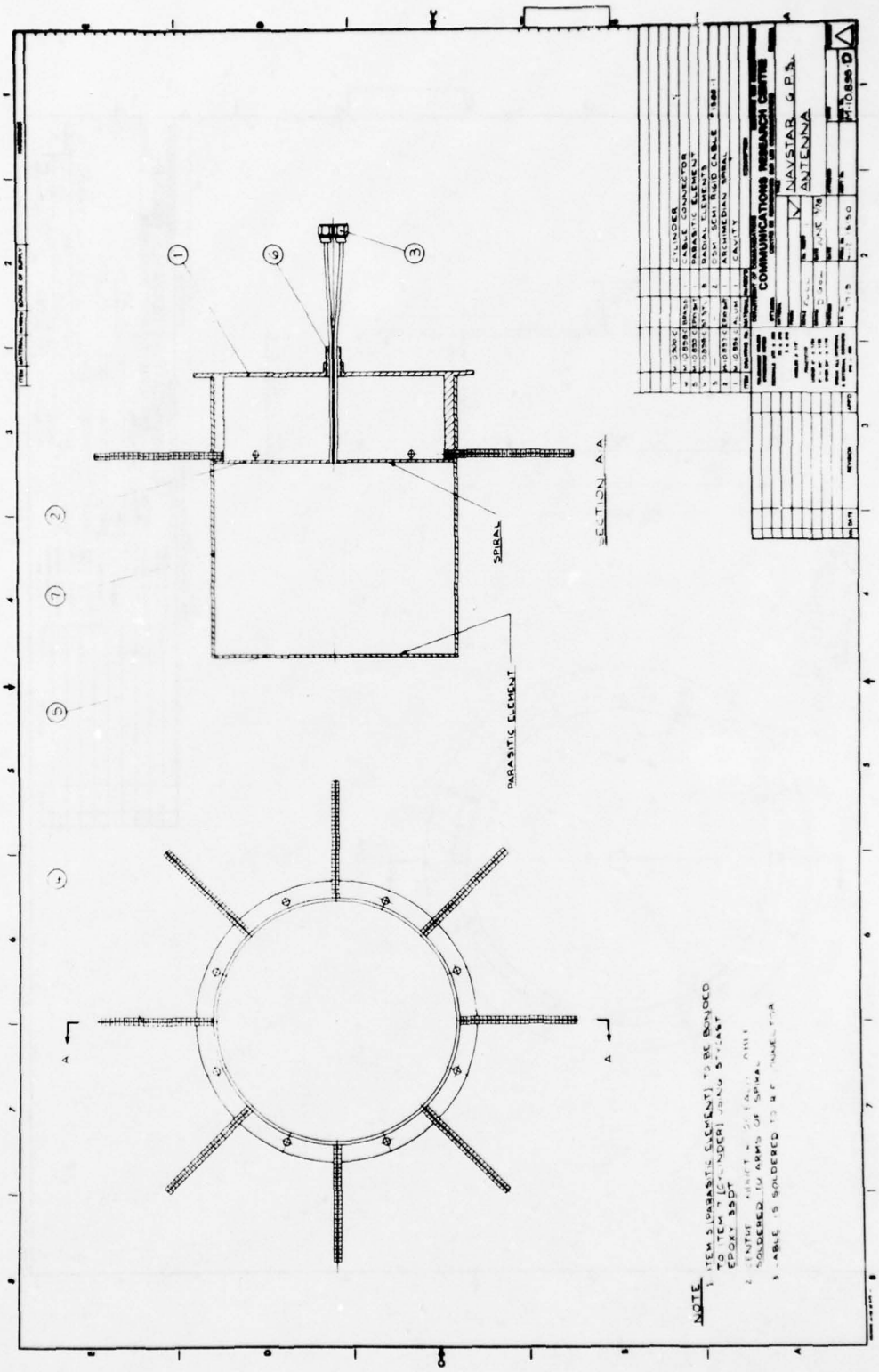

Figure B1. NAVSTAR G.P.S. Antenna

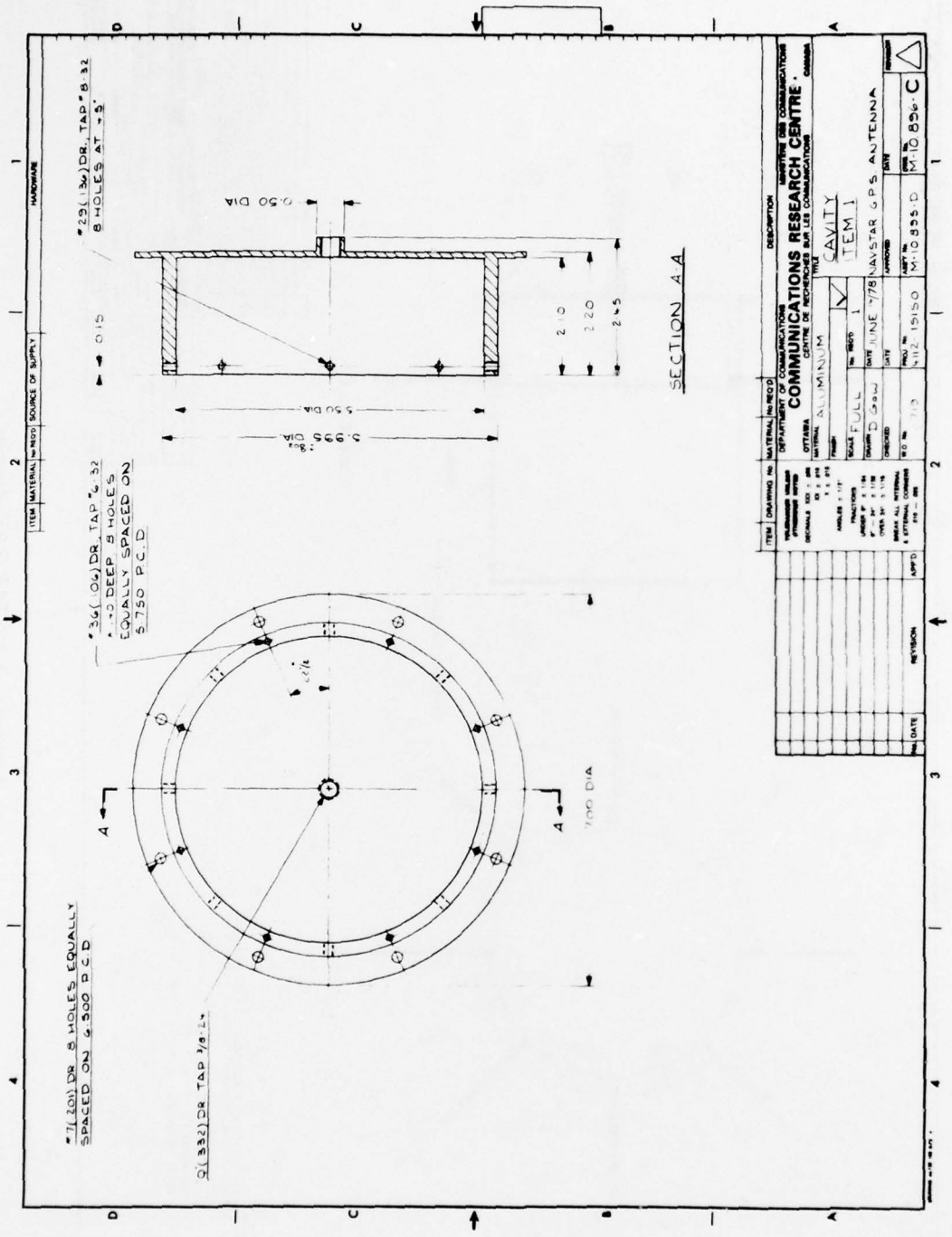

Figure B2. Cavity Item 1

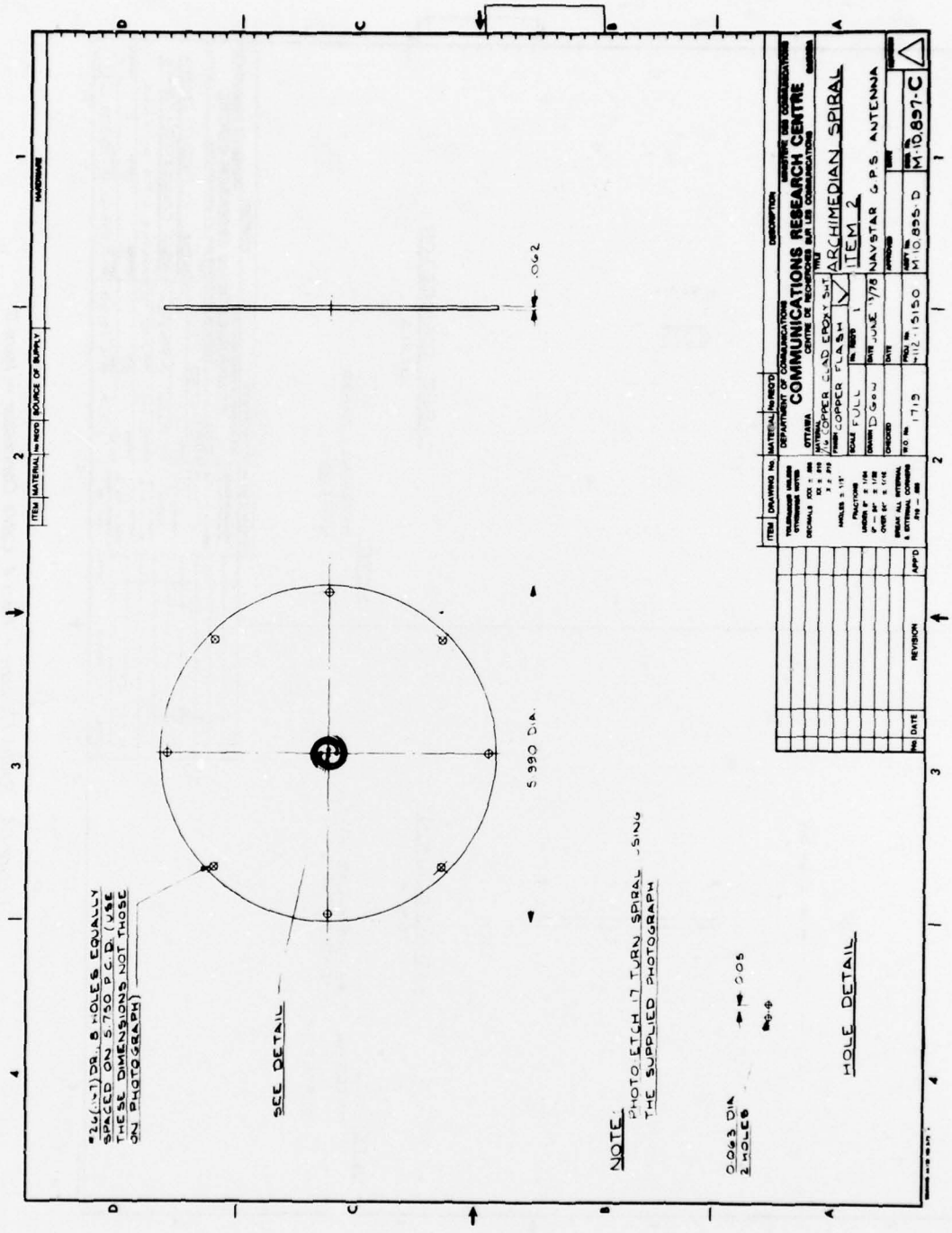

Figure B3. Archimedian Spiral Item 2

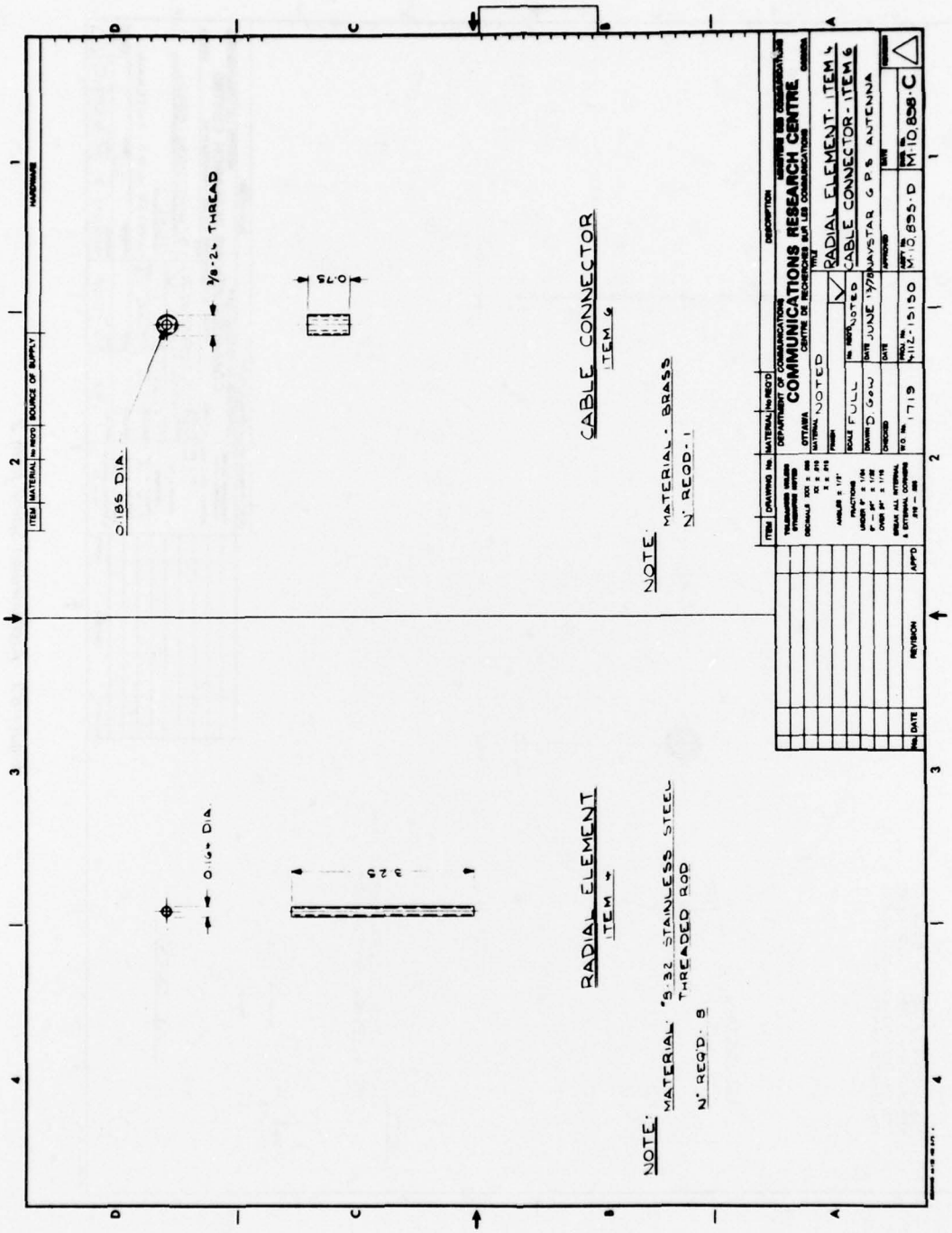

Figure B4. Radial Element – Item 4, Cable Connector – Item 6

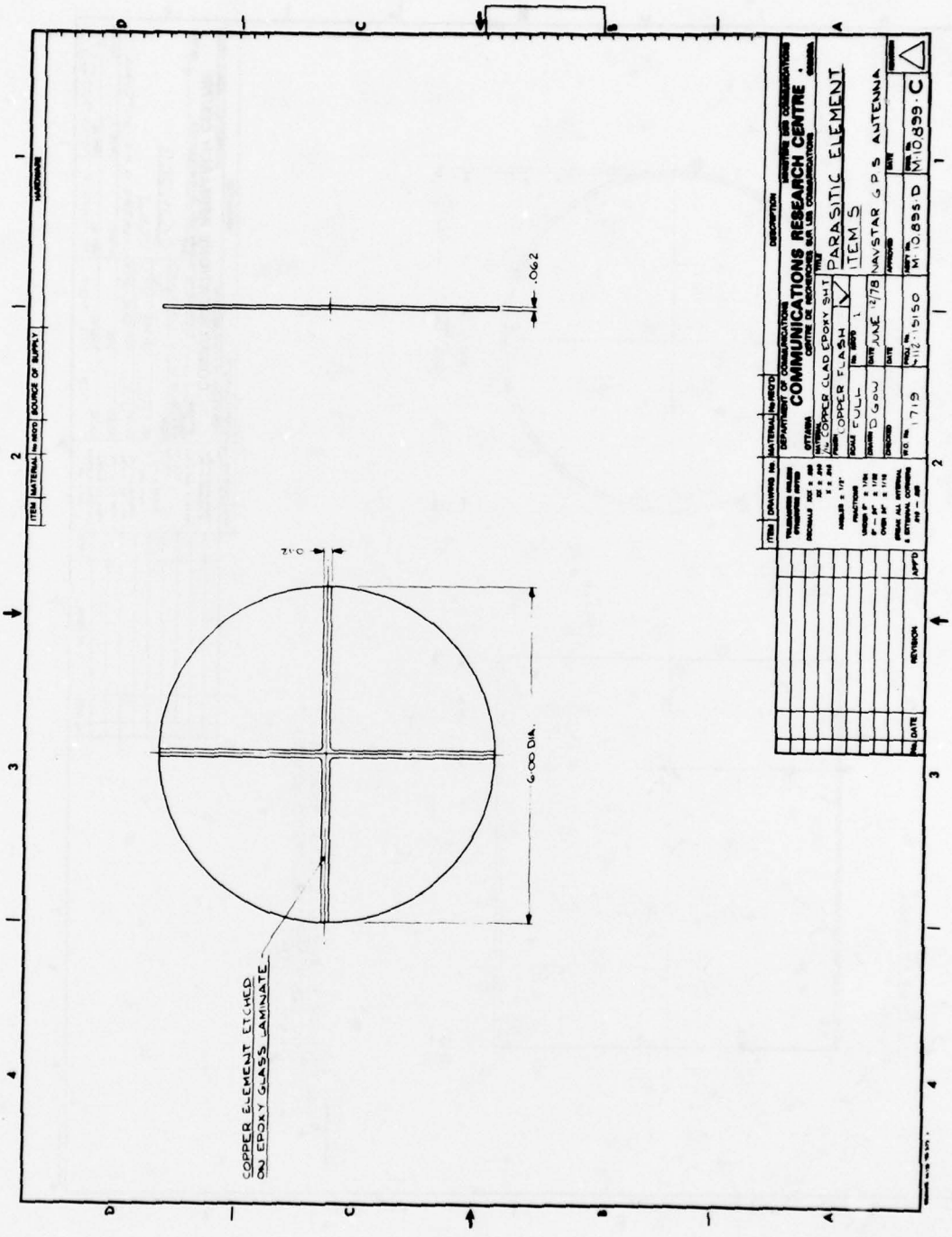

Figure B5. Parasitic Element Item 5

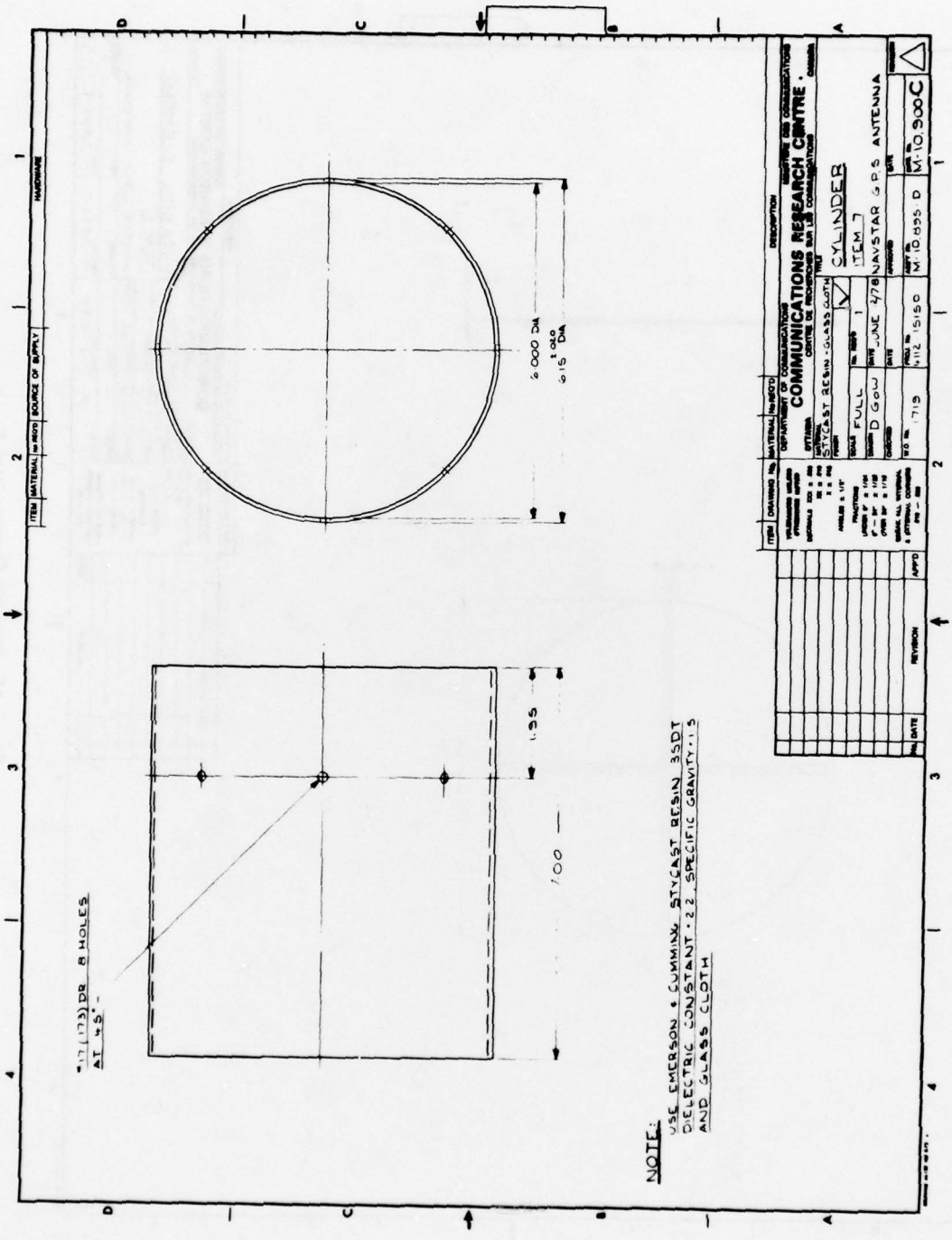

Figure B6. Cylinder Item 7